RSC Advances

PAPER

View Article Online
View Journal | View Issue

Cite this: *RSC Adv.*, 2025, **15**, 8675

RP-HPLC method development and validation for the quantification of prednisolone and salbutamol with their simultaneous removal from water using modified clay–activated carbon adsorbents†

M. Ramadan Mahmoud,[a] Samar M. Mahgoub,[b] Rania Abdelazeem,[c] Mahmoud M. Abdelsatar,[d] Ahmed A. Allam,[ef] Haifa E. Alfassam,[g] Abdelatty M. Radalla[h] and Rehab Mahmoud *[h]

Salbutamol sulfate (SAL) and prednisolone (PRD) are commonly used for treating respiratory and inflammatory conditions, yet they are frequently detected in aquatic ecosystems, posing significant risks to aquatic life and biodiversity. Despite the growing concern over pharmaceutical pollution, there is a lack of reliable and sustainable methods for quantifying these drugs in both pharmaceutical and environmental samples, as well as effective adsorbents for their removal from contaminated water. This study aims to fill this gap by developing a reliable reversed-phase high-performance liquid chromatography (RP-HPLC) method for quantifying SAL and PRD, while also creating an organoclay–activated carbon composite adsorbent for removing these drugs from water. The HPLC method was validated for linearity, precision, accuracy, robustness, and specificity, with detection limits of 1.06 μg mL^{-1} for SAL and 0.95 μg mL^{-1} for PRD. The adsorbent demonstrated high efficiency in removing both drugs, achieving maximum adsorption capacities of 731.64 mg g^{-1} for SAL and 888.75 mg g^{-1} for PRD at pH 7, with an adsorbent dose of 0.4 g and a temperature of 45 °C. Thermodynamic analysis revealed that the adsorption process is both endothermic and spontaneous. Characterization of the adsorbent using FTIR, SEM, XRD, and BET confirmed its effective structure. Adsorption followed the Langmuir model for SAL and the Sips model for PRD, with equilibrium reached within 240 minutes and the process following pseudo-second-order kinetics. Ethanol proved more effective than acetone and acetic acid for desorbing SAL, while acetone was more effective for PRD. The organoclay–activated carbon adsorbent was found to be cost-effective, offering a practical solution for large-scale water treatment. Sustainability assessments using the ComplexGAPI, BAGI, and RGB 12 algorithms highlighted its strong environmental friendliness. This research provides valuable insights for pharmaceutical quality control and the environmental remediation of pharmaceutical pollutants.

Received 13th January 2025
Accepted 23rd February 2025

DOI: 10.1039/d5ra00324e

rsc.li/rsc-advances

1 Introduction

Salbutamol sulphate (SAL) and prednisolone are widely used drugs. SAL acts as a β2-agonist for asthma and COPD, and prednisolone is known for its anti-inflammatory and immunosuppressive properties. Their combination provides synergistic benefits for respiratory and inflammatory conditions (Fig. 1). However, their widespread use raises concerns about environmental impact, especially in aquatic ecosystems. Pharmaceuticals, including salbutamol and prednisolone, have

[a]*Faculty of Pharmacy, Al-Azhar University, Assiut, Egypt*

[b]*Materials Science and Nanotechnology Department, Faculty of Postgraduate Studies for Advanced Sciences, Beni-Suef University, Beni-Suef, Egypt. E-mail: miramar15@yahoo.com*

[c]*Environmental Science and Industrial Development Department, Faculty of Postgraduate Studies for Advanced Sciences, Beni-Suef University, Beni-Suef 62521, Egypt*

[d]*Department of Geology, Faculty of Science, Beni-Suef University, Beni-Suef, Egypt. E-mail: mahmoud.abdelstar.1997@gmail.com*

[e]*Department of Biology, College of Science, Imam Mohammad Ibn Saud Islamic University, Riyadh 11623, Saudi Arabia*

[f]*Department of Zoology, Faculty of Science, Beni-suef University, Beni-suef 65211, Egypt. E-mail: Ahmed.aliahmed@science.bsu.edu.eg*

[g]*Department of Biology, College of Science, Princess Nourah bint Abdulrahman University, P.O. Box 84428, Riyadh 11671, Saudi Arabia. E-mail: halfassam@pnu.edu.sa*

[h]*Chemistry Department, Faculty of Sciences, Beni-Suef University, Beni-Suef, Egypt. E-mail: rehabkhaled@science.bsu.edu.eg; abdelaty.mohamed@science.bsu.edu.eg*

† Electronic supplementary information (ESI) available. See DOI: https://doi.org/10.1039/d5ra00324e

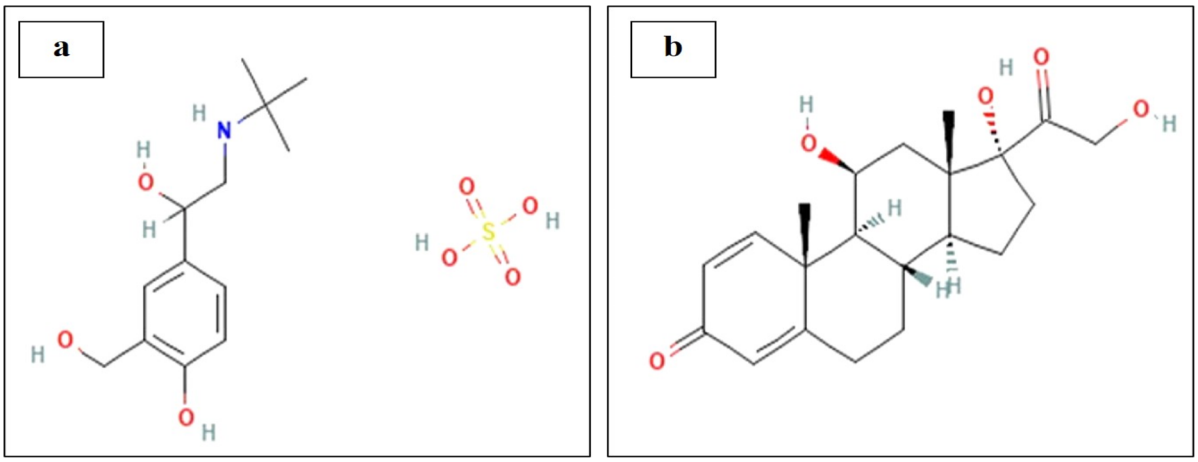

Fig. 1 Chemical structure of (a) SAL, (b) PRD.

been increasingly detected in water bodies, often at trace levels, due to their persistence in the environment and incomplete removal during wastewater treatment processes.[1–3] Recent studies have reported the presence of salbutamol and prednisolone in surface waters at concentrations ranging from ng L^{-1} to μg L^{-1}, with higher levels observed in regions with inadequate wastewater treatment infrastructure.[4–6] The discharge of these drugs into aquatic systems poses ecological risks, with salbutamol disrupting aquatic organisms' behavior, growth, and reproduction by affecting the endocrine system.[4,7] Similarly, prednisolone, a corticosteroid, can alter aquatic biodiversity, affecting the health and development of fish and other aquatic organisms.[8,9] Despite these risks, conventional treatment methods such as activated sludge and chlorination have proven ineffective in completely removing these pharmaceuticals, often leading to the formation of toxic by-products.[10] In the study region, the lack of advanced treatment facilities exacerbates the problem, resulting in persistent contamination of water sources with these compounds.[11,12] These negative effects highlight the urgent need for effective methods to remove pharmaceutical pollutants from water sources.

The study addresses the dual challenge of quantifying salbutamol sulphate and prednisolone in pure and pharmaceutical forms while also addressing their environmental impact as water contaminants. A robust RP-HPLC method ensures precise quantification of these drugs in pharmaceuticals and environmental samples. Additionally, we propose a novel adsorbent material for their effective removal from contaminated water. While bentonite/activated carbon composites have been extensively studied for water treatment applications, their use for the simultaneous removal of salbutamol and prednisolone remains underexplored, particularly in the context of the study region.[13,14]

Organoclay, a chemically modified form of natural bentonite or other smectite clays, is highly effective in water treatment. The modification involves intercalating organic cations, enhancing its ability to adsorb hydrophobic pollutants. This process increases surface area and improves adsorption properties, making organoclay a valuable material for pollutant removal.[15] Its unique properties, such as high surface area, strong adsorption capacity, thermal stability, and chemical resistance, make it an ideal choice for removing a wide range of pollutants and treating pharmaceutical contaminants in water.[15–17] To improve water treatment efficiency, activated carbon (AC) is combined with organoclay to create a composite adsorbent. AC, known for its high porosity and extensive surface area, is derived from materials like bamboo, coconut husk, wood, coal, and petroleum pitch.

According to their properties, it is also utilized in a variety of applications, including medicine, metals recovery, water purification, biogas purification, and air emission purification. The combination of organoclay with activated carbon will significantly enhance adsorption performance due to the synergistic interaction between the two materials.[18] This approach builds on the well-documented efficacy of bentonite/activated carbon composites in removing organic pollutants, while addressing the specific challenge of pharmaceutical removal.[19–21] When used as a composite adsorbent, organoclay can act as a pretreatment stage, capturing larger hydrophobic molecules and reducing the load on AC. This synergy enhances the overall removal efficiency of pharmaceutical contaminants, ensuring cleaner and safer water. Additionally, this combination can extend the lifespan of the filtration system and reduce operational costs. The synthesis of an organoclay–activated carbon composite adsorbent was studied for removing salbutamol sulphate and prednisolone from water. The adsorption process was assessed using a developed RP-HPLC method, ensuring reliable efficiency evaluation. Results indicate that activated carbon enhances organoclay's adsorptive capacity, offering an effective solution for pharmaceutical pollutant removal (Scheme 1). This study integrates accurate quantification techniques with an innovative adsorbent, contributing to both environmental remediation and advanced water treatment technologies. Table S1† compares the performance of the proposed HPLC method with recent publications for SAL and PRD determination.

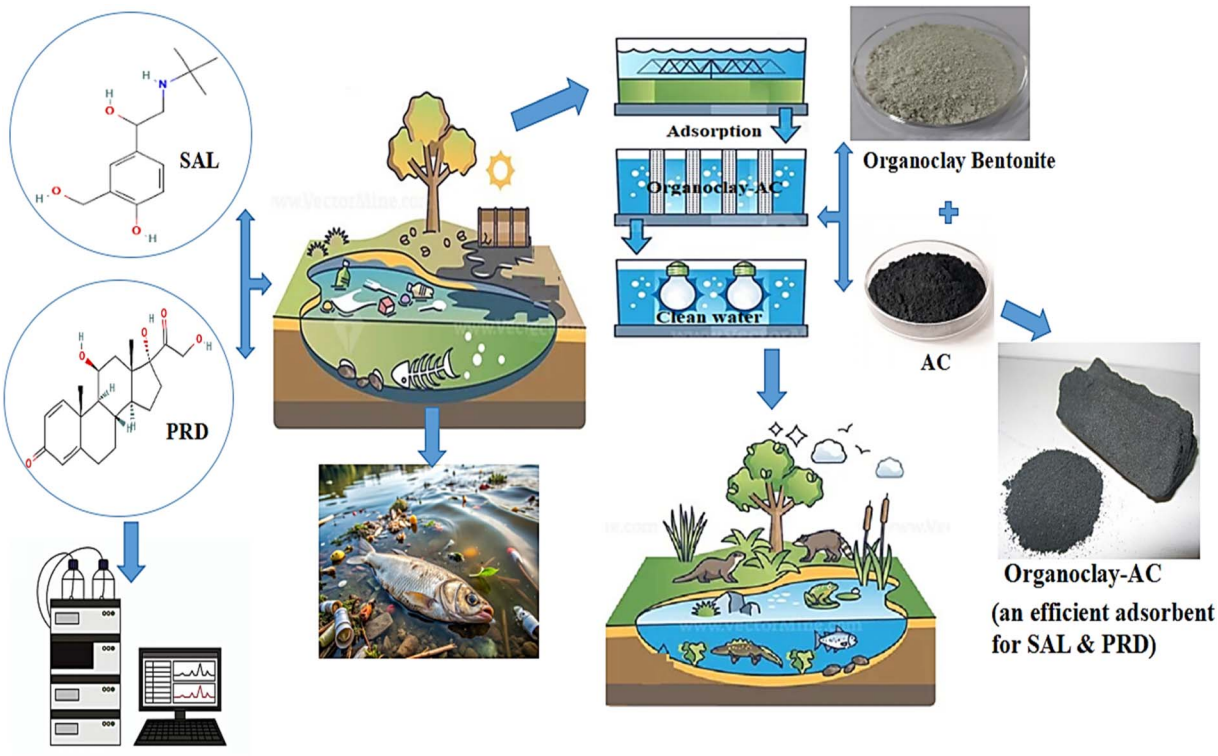

Scheme 1

2 Materials and methods

2.1. Chemicals and reagents

Perchloric acid, ethanol and acetonitrile were obtained from fischer. Salbutamol sulphate (purity 99.72%) was purchased from Arshine Pharmaceutical Co., Limited, Changsha, China. Whereas prednisolone (purity 98.97%) was purchased from Zhejiang, China. SAL and PRD were obtained from local pharmacies with valid expiration dates as commercially available tablets. Activated carbon, hydrochloric acid and absolute ethanol 99% were purchased from Scharlau (Barcelona, Spain). Sodium hydroxide was purchased from Emsure (Darmstadt, Germany). Bentonite organoclay is a type of organoclay derived from bentonite, a naturally occurring clay mineral primarily composed of montmorillonite. Bentonite organoclay is created by modifying the surface of bentonite with organic compounds, typically quaternary ammonium salts or surfactants, to make it more compatible with organic materials acting as an effective adsorbent for pharmaceutical pollutants in wastewater; was purchased from Shanghai Innovy Chemical New Materials Co., Ltd (Zhejiang, China). Bi-distilled water of analytical grade was used.

2.2. Chromatographic analysis and studies

Agilent HPLC 1200 series System (California, USA) is designed to separate complicated materials with high resolution and sensitivity. It has a quaternary-pump configuration for sophisticated LC workflows. Solution A was prepared by adding 1 mL of perchloric acid in 1000 mL distilled water. Solution B is acetonitrile. Then mobile phase is prepared as a mixture of solution A and solution B with ratio 33 : 67. Diluent was bidistilled water. The chromatographic system was configured for isocratic mode RP-HPLC. An Inertsil ODS 3V column of specification (4.6 × 250 mm, 5 μm) was used. The sample and column oven temperatures were set to 5 °C and 40 °C, respectively. The mobile phase is prepared as a mixture of solution A and solution B with ratio (33 : 67, v/v). The RP-HPLC method had a three-minute runtime, a 10.0 μL injection volume, a 2 mL min^{-1} flow rate, and 214 nm UV detection.

2.3. Adsorbent synthesis

Two grams of bentonite organoclay were added to one gram of activated carbon in 100 mL of bidistilled water. The mixture was sonicated for 30 minutes, followed by centrifugation to separate the supernatant from the formed adsorbent. The adsorbent was then washed three times with distilled water, followed by ethanol. Finally, the adsorbent was dried in an oven at 70 °C for 12 hours until completely dry.

2.4. Characterization of the adsorbent

The properties of the formed adsorbent were analyzed using several techniques, including FTIR spectroscopy. Samples including the organoclay and that of organoclay after pollutants adsorption, were analyzed to get the IR spectra using a Bruker Vertex 70 spectrometer (Germany) in the range of 4000–400 cm^{-1}. In addition to FTIR, the adsorbent and the composite were examined using SEM to assess their surface morphology and chemical composition. Also, X-ray diffraction (XRD)

investigation was conducted using Panalytical (Empyrean) X-ray diffractometer with Cu-Kα radiation (wavelength 0.154 nm) that operated at a current of 35 mA and voltage of 40 kV, scanning at a rate of 8° min^{-1} from 5° to 80° (2θ).

2.5. Adsorption study

The batch adsorption method was employed in this study. Stock solutions of salbutamol (SAL) and propranolol (PRD) were prepared at a concentration of 1000 μg mL^{-1} using 50% ethanol, and serial dilutions (using bidistilled water as a diluent) were made to construct calibration curves for each drug. Various factors influencing the adsorption process were examined, including adsorbent dose, pH, drug concentrations, temperature, and contact time between the adsorbent and pollutants. To investigate the pH effect, 0.1 g of the prepared adsorbent was added to five Falcon tubes (50 mL), followed by the addition of 100 μg mL^{-1} SAL and PRD solutions, and the tubes were filled with distilled water. The pH was adjusted to 3, 5, 7, 8, and 9 using 0.1 N NaOH or 0.1 N HCl. The tubes were placed on an orbital shaker at 200 rpm overnight. For examining the adsorbent dose, different doses were added to five more Falcon tubes containing solutions adjusted to the optimal pH. Each dose was tested in triplicate, and average results were recorded. The doses tested were 0.075 g, 0.1 g, 0.2 g, 0.4 g, and 0.5 g. Drug concentration effects were studied in the range of 5–500 μg mL^{-1} under the optimal conditions. The temperature's influence on the adsorption process was tested at 15, 25, 30, 35, and 45 °C, and the thermodynamic parameters were calculated. The Point of Zero Charge (PZC) of the organoclay was determined by adding 0.1 g of the adsorbent to 25 mL of aqueous solutions at various pH levels (3, 5, 7, 8, 9, and 10). The solutions were equilibrated for 24 hours to stabilize at a final pH. The PZC was identified as the initial pH where the change in pH (ΔpH) was zero. Quantitative sorption was performed using high-performance liquid chromatography (HPLC), while the adsorption process was further evaluated through isotherms and kinetics studies.

2.6. Regeneration of adsorbent

In this study, the regeneration of organoclay was explored by using a 1.0 g L^{-1} SAL–PRD-loaded adsorbent with various regeneration agents, such as ethanol, acetone, and acetic acid. Each agent was prepared at a 50% v/v concentration in 20 mL of solution. Desorption experiments were performed in batch reactors, operating for 1 hour at 140 rpm and 30 °C. To evaluate the efficiency of the regenerated organoclay, multiple adsorption–desorption cycles were conducted to determine its capacity for removing SAL–PRD. The performance of the regenerated organoclay was calculated using eqn (1):

$$\text{Percentage removal } (\%) = \frac{(C_0 - C_f) \times 100}{C_f} \quad (1)$$

where C_0 is the initial concentration of SAL and PRD (mg L^{-1}), C_f is the final concentration of SAL and PRD (mg L^{-1}).

3 Results and discussion

3.1. Methods development and optimization

The optimal flow rate of 2 mL min^{-1} was determined by testing rates from 0.5 to 2 mL min^{-1}. Various columns (C8, C18, phenyl, and cyano) were evaluated, with the Inertsil ODS 3V column (4.6 × 250 mm, 5 μm) chosen for its superior performance. Scanning wavelengths between 200 and 400 nm were tested, with the best resolution at 214 nm, matching the analyte's absorption. Different mobile phase compositions, including methanol/water (30 : 70 v/v), acetonitrile/water (50 : 50 v/v), and pH-adjusted phosphate, were assessed. The most effective mobile phase was solution A (1 mL perchloric acid in 1000 mL distilled water) and solution B (acetonitrile) at a 33 : 67 ratio, successfully separating SAL and PRD with sharp peaks. The column oven was set to 40 °C to enhance mass transfer, separation, and reproducibility, as shown in Fig. 2.

3.2. Method validation

The methodologies we proposed have been validated according to the ICH criteria. The results demonstrate that these strategies are both effective and dependable for analysts.[22]

3.2.1. Linearity, limit of detection (LOD), and limit of quantification (LOQ). A calibration curve for each drug was constructed by plotting peak area *versus* concentration. Serial dilutions of a 1000 μg mL^{-1} stock solution were prepared in duplicate within the concentration range of 3–50 μg mL^{-1}, as

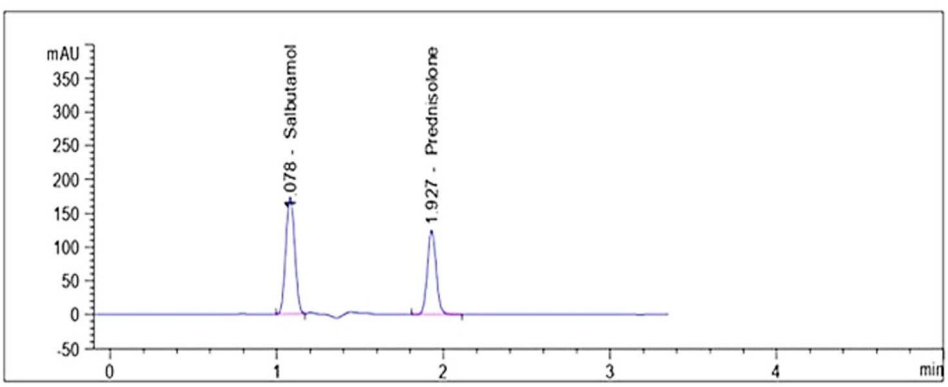

Fig. 2 HPLC chromatograms of SAL and PRD recorded at the optimum wavelength of 214 nm.

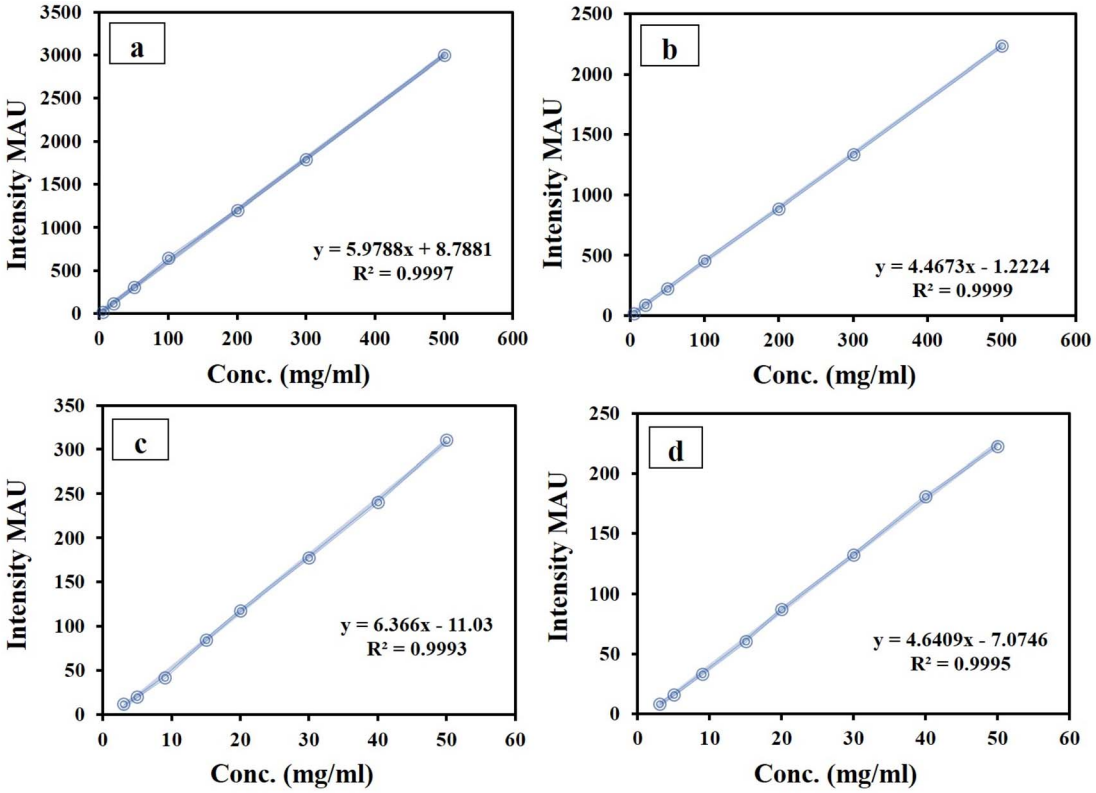

Fig. 3 (a and b) Calibration curves for determination of SAL and PRD and (c and d) calibration curve at low concentrations for determination of LOQ and LOD of SAL and PRD.

shown in Fig. 3a–d. Regression analysis data, including slope, intercept, and R^2 values, are provided in Table 1. The limits of detection (LODs) and quantification (LOQs) were determined using the formulas (3.3/S) and (10/S), based on the standard deviation of the y-intercept and the slope of the calibration curve, as calculated in a validated Excel spreadsheet. Table 1 also highlights the inverse relationship between sensitivity and the corresponding LOD and LOQ values for the proposed methods.

3.2.2. Precision. We conducted comprehensive intraday and interday evaluations by performing six measurements over three consecutive days to assess the method's repeatability and intermediate precision, as detailed in Table 2. The relative standard deviation (RSD) was calculated using the formula RSD = (SD × 100)/mean. The results indicated an RSD of less than 2%, confirming that the precision of the developed method is excellent.

Table 1 Regression and statistical parameters from the calibration curves of SAL and PRD[a]

	Drugs	
Parameter	SAL	PRD
Wavelength	214 nm	214 nm
Range (μg mL^{-1})	3–50	3–50
Coefficients of determination (R^2)	0.9993	0.9995
Slope	6.366	4.6409
Intercept	−11.03	−7.0746
LOD	1.06 μg mL^{-1}	0.95 μg mL^{-1}
LOQ	2.87 μg mL^{-1}	2.11 μg mL^{-1}

[a] Limit of detection (3.3 × σ/slope) and a limit of quantitation (10 × σ/slope).

3.2.3. Accuracy and recovery. Triplicate 10 μL injections were made for each concentration level of the sample (50%, 100%, and 150%) relative to the standard analyte concentration. The recovery test results indicate the consistency between the actual and measured values, with these calculations based on the experimental data shown in Table 3.

3.2.4. Robustness. Robustness refers to the method's ability to remain reliable despite small, intentional changes in its parameters. To evaluate this, standards were prepared and injected after modifying each drug parameter. Table 4 displays various modifications, such as adjustments in wavelength (214 nm ± 2 nm), flow rate (2 mL min^{-1} ± 0.1 mL min^{-1}), and the mobile phase composition ratio (solution A% ± 1%).

3.2.5. System suitability. The system suitability tests were conducted according to standard laboratory calculations outlined in the United States Pharmacopeia guidelines.[23] Critical factors that must fall within defined limits to ensure the system's suitability include the resolution between two adjacent peaks, which must be at least 2; the number of theoretical plates, reflecting column efficiency, which should be greater than 2000; and the tailing or asymmetry factor, which should not exceed 2 ($T \leq 2$), as outlined in Table 5.

Table 2 Results of assay precision test for SAL and PRD in the marketed formulations

	SAL		PRD	
Test	1st analyst (within a day)	2nd analyst (between 3 consecutive days)	1st analyst (within a day)	2nd analyst (between 3 consecutive days)
Test 1	100.11	100.20	100.55	100.44
Test 2	100.18	100.22	100.42	100.52
Test 3	100.23	100.26	100.50	100.41
Test 4	100.22	100.31	100.46	100.55
Test 5	100.09	100.24	100.53	100.35
Test 6	100.15	100.22	100.45	100.40
Average	100.16	100.24	100.49	100.44
SD	0.05	0.04	0.05	0.07
RSD	0.05	0.04	0.05	0.07
Pooled RSD (12 samples)	0.06		0.06	

Table 3 Results of accuracy for SAL and PRD in the marketed formulation

		SAL			PRD		
Test %	St add.n (mL) to 20 mL flask	Calculated amount μg mL^{-1}	Amount found μg mL^{-1}	Recovery %	Calculated amount μg μg mL^{-1}	Amount found μg μg mL^{-1}	Recovery %
50%	5	25.25	25.27	100.07	20.30	20.35	100.24
100%	10	50.50	50.49	99.98	40.60	40.95	100.86
150%	15	75.75	75.80	100.07	60.9	61.23	100.54
Minimum				99.98			100.24
Maximum				100.07			100.86
Average				100.02			100.54
SD				0.06			0.31
RSD%				0.06			0.30

Table 4 Method robustness for the developed method

		Wavelength (nm)		Solution A% ratio		Flow rate	
Analyte	Chromatographic parameters	212	216	32%	34%	1.9 min mL^{-1}	2.1 min mL^{-1}
SAL	Assay %	100.05%	100.00%	99.98%	100.06%	100.07%	99.89%
	Retention time (R_t)	1.066	1.070	1.082	1.071	1.086	1.065
	Tailing factor	0.93	0.92	0.93	0.90	0.94	0.91
	Resolution	N/A	N/A	N/A	N/A	N/A	N/A
PRD	Assay %	100.38%	100.41%	100.33%	100.24%	99.95%	100.19%
	Retention time (R_t)	1.96	1.98	2.03	1.85	2.04	1.81
	Tailing factor	0.91	0.93	0.92	0.93	0.94	0.92
	Resolution	8.55	8.52	8.54	8.52	8.56	8.54

Table 5 Results of system suitability parameters for SAL and PRD

Suitability parameter	SAL	PRD	Limit
Retention time	1.078	1.927	$R_t \pm 10\%$
Resolution	N/A	8.52	NLT 2.0
Theoretical plates	2862	6316	NLT 2000
Tailing factor	0.93	0.91	NMT 2.0%

3.2.6. Selectivity. This method evaluates the selectivity of our developed approach in determining the contents of salbutamol and prednisolone without interference from solvents or excipients. The selectivity study involved injecting placebo and matrix samples into the HPLC system to observe their effect on the main peaks, as illustrated in Fig. 4a and b.

3.3. Adsorption studies

3.3.1. Material characterization. The X-ray diffraction (XRD) patterns obtained from the OC/AC adsorbent reveal a diverse mineralogical composition, as illustrated in Fig. 5a. The organoclay (OC) is comprised of several minerals, including quartz, feldspars, and montmorillonite, which are a direct consequence of its environmental origins. The presence of montmorillonite, with the chemical formula $(Na, Ca)_{0.3}(Al,$

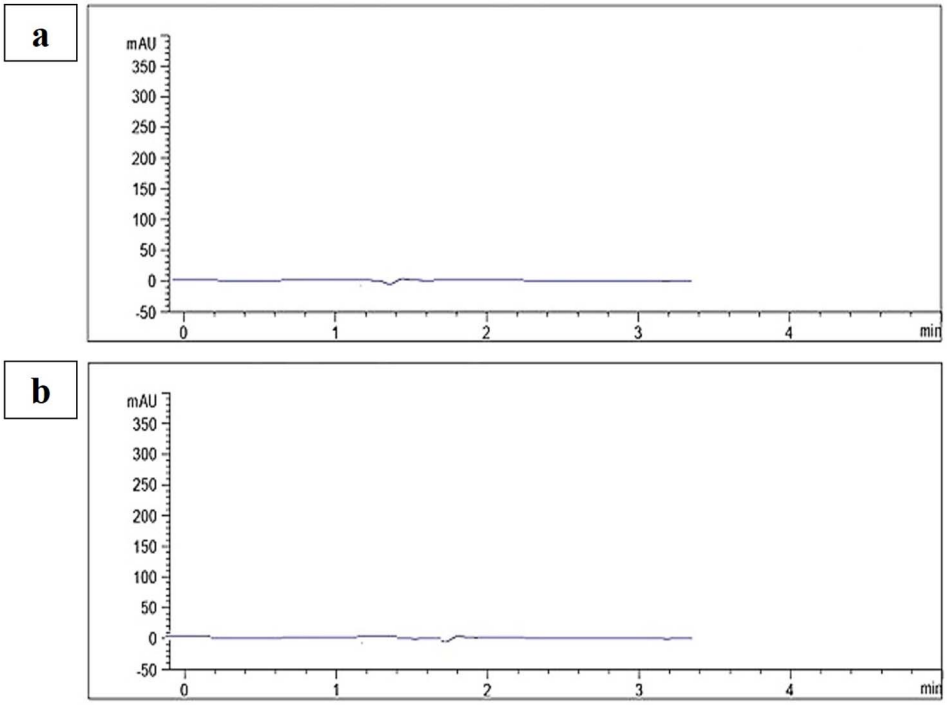

Fig. 4 Chromatograms of (a) diluent, (b) placebo recorded at the optimum wavelength of 214 nm.

$Mg)_2Si_4O_{10}(OH)_2 \cdot nH_2O$, was confirmed through the identification of characteristic diffraction peaks. These peaks were observed at 2θ values of 20.58°, 30.02°, 35.54°, 56.08°, 62.75°, and 74.40°, which correspond to the JCPDS file (card no. 13-0135).[14–16] Additionally, typical peaks corresponding to quartz (SiO_2) were identified at 2θ values of 27.15°, 46.33°, 50.90° (JCPDS no. 46-1045), and 68.93°. Furthermore, peaks for feldspars, represented by the formula (K, Na)$AlSi_3O_8$–$CaAl_2Si_2O_8$, were recognized at 12.89°, 25.49°, and 28.36° (JCPDS no. 70-1862).[17–19] The amorphous nature of AC results in the absence of distinct diffraction peaks,[24] this behavior may also apply to the organic matter present within the internal structure of OC. Consequently, it is essential to employ additional analytical techniques, such as FTIR and FESEM, to accurately identify the organic components.

The FTIR spectrum of the OC/AC adsorbent is presented in Fig. 5b. Notably, the modified composite displays a significant absorption band at 3608.36 cm^{-1}, which is indicative of the O–H functional group present within the internal structure of the montmorillonite mineral. The spectrum reveals a band at 3440.44 cm^{-1}, which corresponds to the O–H stretching frequencies associated with silanol groups (Si–O–H). Additionally, another band observed at 1631.44 cm^{-1} represents the bending vibration of water molecules (H–O–H) in a physical state (as adsorbed on montmorillonite's surface). The absorbance bands detected at 2838.10 cm^{-1} and 1427.10 cm^{-1} are linked with the stretching frequencies of $-CH_2$ groups, which may be accompanying to the presence of organic matter within OC.[25] Moreover, the peak at 2372.10 cm^{-1} is indicative of C=C groups of AC, whereas the peak at 2105.92 cm^{-1} is connected with the stretching vibrations of C=N bonds within AC internal structure.[26] The existence of SiO_4^{2-} tetrahedral structures is confirmed by the detection of bending vibrations and stretching bands at wavelengths of 444.86, 518.31, 771.39, and 994.86 cm^{-1}.[27] Also, the AlO_4 octahedral units within the internal structure of montmorillonite are situated at approximately 774 cm^{-1}.[28] Following the adsorption of the prednisolone and salbutamol, new absorption peaks were detected at 2959.35 and 2851.32 cm^{-1}, corresponding to C–H stretching vibrations,[29] as well as at 3813.42 cm^{-1}, which is associated with N–H stretching bonds.[30] Additionally, significant shifts in the intensities and wavenumber values were recognized for the AlO_4 octahedral units, Si–O–H, H–O–H, $-CH_2$, and various SiO_4^{2-} tetrahedral functional groups. The emergence of new peaks and the alteration of the composite spectrum following the adsorption experiment can be attributed to the interactions between the molecules of these pollutants and the functional groups of OC/AC adsorbent, thereby elucidating the mechanisms underlying the effective removal process for these hazardous compounds.

Fig. 6 illustrates the FESEM images of the OC/AC adsorbent captured at various magnifications. The FESEM micrographs clearly demonstrate that the synthesized product exhibits a uniform flaky morphology characterized by a sheet-like structure. Additionally, the microstructure reveals a range of particle sizes along with a rough and porous surface morphology, as depicted in Fig. 6a–c. The composite also demonstrates notable aggregated clusters, which may enhance

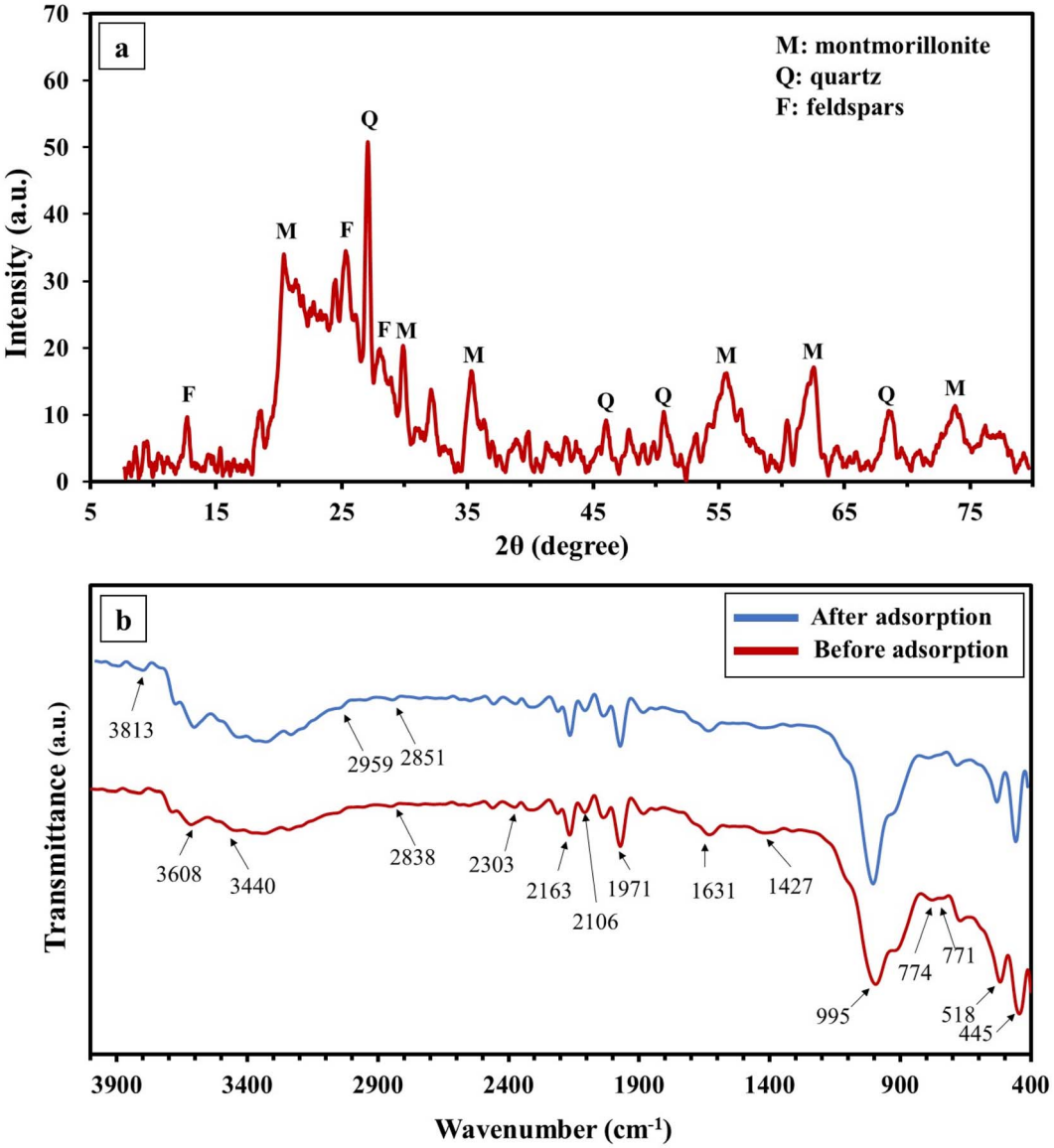

Fig. 5 (a) XRD-analysis of OC/AC composite and (b) FTIR spectrum of OC/AC before and after adsorption.

the insertion of the pollutants into the inner surface of the clay mineral, thereby improving the adsorption process. Afterwards the incorporation of AC into the clay montmorillonite, the surface texture of the clay became markedly rougher, as illustrated in Fig. 6d–f. This phenomenon can be assigned to the insertion of AC within the lattice planes of montmorillonite clay, which possesses a relatively large *d*-spacing (the distance between clay planes) compared to other clay types. Furthermore, the FESEM images indicate that AC functions as a coating material and/or substrate on the clay surface. These morphological alterations result in a significant increase in surface irregularity, leading to a more asymmetrical surface and enhanced porous structure. As a consequence, this improvement may augment the overall surface area of the as-synthesized composite, thereby increasing the material's adsorption capacity for the pollutants under investigation.

Fig. 7 illustrates the outcomes of N_2 adsorption–desorption isotherms of the OC/AC composite providing essential insights into its internal structural characteristics. The surface area and average pore diameter of the OC/AC composite were determined to be 720.493 $m^2\ g^{-1}$ and 3.53 nm, respectively. The graph depicting the relationship between relative pressure (P/P_0) and the quantity adsorbed ($cm^3\ g^{-1}$) in Fig. 8 illustrates a Type IV N_2 adsorption/desorption isotherm, as classified by the International Union of Pure and Applied Chemistry (IUPAC). The presence of a Type IV hysteresis loop indicates that the developed OC/AC adsorbent possesses a range of pore sizes, predominantly consisting of mesopores and micropores. The pore volume of the synthesized binder, measured at 0.578 $cm^3\ g^{-1}$, suggests that the adsorbed pollutants may diffuse more efficiently, potentially enhancing the removal capacity. The data presented above show a significant

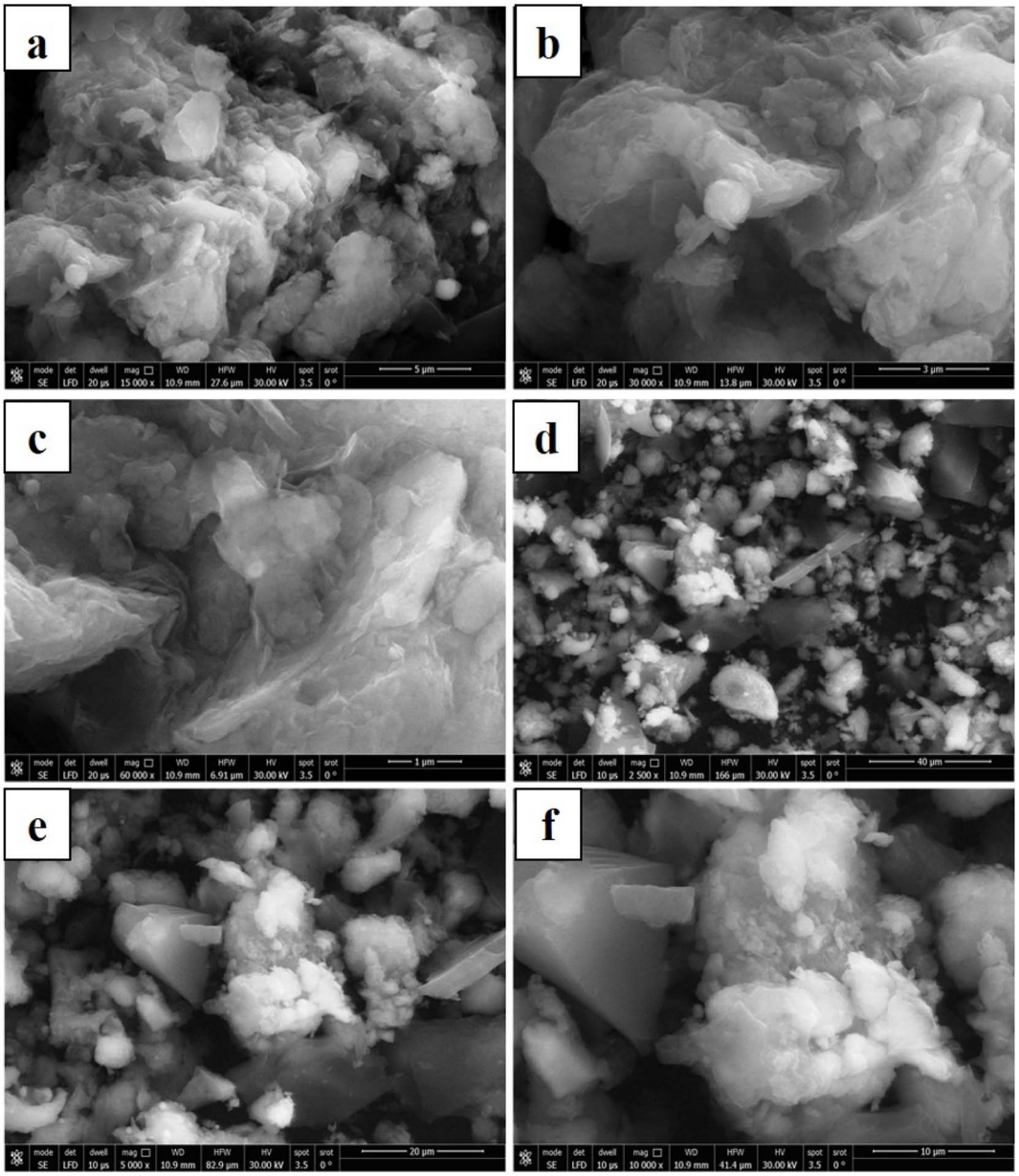

Fig. 6 FESEM spectrum of OC/AC adsorbent (a–f).

correlation with the FESEM results (Fig. 7), which explain a complex and aggregated surface morphology characterized by irregular porous phases, high surface area, and a nanoporous structure.

3.3.2. Effect of pH, dose of adsorbent and temperature. The adsorption of SAL and PRD on the organoclay–activated carbon composite is influenced not only by pH and adsorbent dose but also by the pK_a values of the drugs, which govern their ionization behavior in solution. The pK_a values of the drugs play a crucial role in determining the ionic form of the molecules, which in turn affects their interaction with the adsorbent surface.[31,32] SAL has a pK_a value of 9.1,[33] meaning that at pH values below this, the drug predominantly exists in its cationic form, while at pH values above this, it becomes largely neutral or slightly anionic, Fig. 8a. PRD, on the other hand, has a pK_a of 12.5,[34,35] indicating that it exists primarily in its neutral form at most environmental pH values, but at very high pH, it may ionize slightly to anionic species, Fig. 8b.[31]

Given the PZC of the organoclay adsorbent is 6.2, Fig. 8c, the surface charge of the adsorbent becomes neutral at this pH, enhancing the interaction with both drugs. At pH 7, both SAL and PRD exhibit favorable adsorption: SAL is in a partially cationic form, which can interact with the surface of the adsorbent that may carry a small negative charge at this pH, while PRD, existing mostly in its neutral form, interacts through van der Waals forces and hydrogen bonding. At lower pH values (such as 3 and 5), the cationic form of SAL is more prevalent, but the positive charge of the adsorbent at these pH values may lead

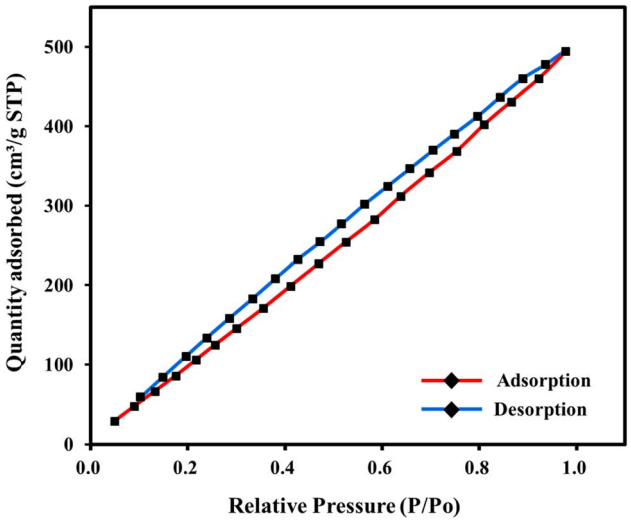

Fig. 7 The adsorption–desorption isotherms of N_2 for OC/AC at 77 K.

to repulsion, reducing adsorption efficiency. At higher pH values (8 and 9), the ionic form of SAL may further increase, leading to weaker interactions with the adsorbent. Similarly, at these pH levels, PRD may undergo slight ionization, but it remains predominantly neutral, limiting any additional interaction with the adsorbent surface.

Regarding the adsorbent dose, a dose of 0.4 g was found to achieve the maximum adsorption capacity for both SAL and PRD. Increasing the dose beyond this resulted in no significant enhancement of adsorption efficiency, as the adsorbent's active sites became saturated. This phenomenon aligns with general adsorption principles, where adsorption increases with the amount of adsorbent until the surface sites are fully occupied, after which further increases in dose have no impact, Fig. 8a and b.[36,37] The temperature plays a crucial role in the adsorption process of SAL and PRD onto organoclay–activated carbon composites. To evaluate its effect, experiments were conducted at different temperatures (15 °C, 25 °C, 30 °C, 35 °C, and 45 °C). The results revealed that the adsorption efficiency of both SAL and PRD increased as the temperature rise, with the highest removal efficiency observed at 45 °C. This trend is consistent with other studies, which indicate that higher temperatures enhance the diffusion rate of the pollutants to the adsorbent surface and improve the interactions between adsorbate molecules and the adsorbent, Fig. 9a–d.[38,39]

The adsorption process was determined to be endothermic, meaning it requires heat to proceed, as demonstrated by the increase in adsorption capacity with temperature. This behavior is typical of adsorption processes where elevated temperatures help overcome energy barriers and facilitate the movement of molecules into the pores of the adsorbent.[40,41] Thermodynamic parameters were calculated to further support these findings. The Gibbs free energy (ΔG) values showed highly negative values at higher temperatures, indicating that the adsorption process becomes more spontaneous as the temperature increases.[42] Moreover, the entropy change (ΔS) was positive for both drugs, suggesting that the adsorption process leads to an increase in disorder within the system. This is a typical characteristic of endothermic reactions, where both the adsorbate and adsorbent gain more freedom of movement.[43]

3.3.3. Adsorption isotherm and kinetics investigation. This study investigated the adsorption of both SAL and PRD onto the synthesized adsorbent using various non-linear isotherm models: Langmuir, Freundlich, Langmuir–Freundlich, Sips, Redlich–Peterson, Toth, and Baudu, Fig. 10. These models were employed to analyze the equilibrium data and gain insights into the adsorption mechanism. All the tested isotherm models demonstrated excellent fit to the experimental data, with high correlation coefficients (R^2) exceeding 0.99 for both SAL and PRD as shown in Table 6. This suggests that the adsorption process is complex and involves multiple interactions between the adsorbate and the adsorbent surface. The maximum adsorption capacity (q_{max}) was higher for PRD than SAL in the Langmuir model, suggesting a stronger affinity of PRD for the adsorbent. According to the R^2 values offered in Table 6, both the Freundlich and Langmuir models exhibited a robust fit for the adsorption systems of PRD and SAL, with R^2 values nearing unity. To identify the most appropriate classical model, the chi-square (χ^2) values presented in Tables 7 and 8 were examined. The results indicate that the Langmuir model offered the optimal fit for the isotherm data at 25 °C, as demonstrated by the lowest recorded χ^2 values. Consequently, the removal of both PRD and SAL can be attributed to the analogous functional groups present on the synthesized OC/AC adsorbent. These functional groups facilitated the formation of a monolayer of PRD and SAL molecules at the interface between the adsorbent and the adsorbate surfaces. The Langmuir model assumes one layer adsorbed onto a homogeneous surface with a finite number of identical adsorption sites.[44] The results suggest that the synthesized adsorbent exhibits a high affinity for both pollutants and that the adsorption process is likely a complex interplay of various mechanisms. The maximum adsorption capacity (q_{max}) was found to be 731.64 mg g^{-1} for SAL and 888.75 mg g^{-1} for PRD. The equilibrium adsorption constant (K_L) was determined to be 0.004 for SAL and 0.0036 for PRD.

The statistical analysis showed that the three-parameter isotherm Toth and Langmuir–Freundlich had the best correlation with the experimental data across the whole concentration range in the case of the two pollutants. This was because the error functions that were established by the statistical analysis had the highest coefficient of determination (R^2), which was nearly equal to one, and the lowest values. HYBRID and the χ^2 were considered universal indicators that provided the greatest match to the experimental data for isotherm modeling prediction in sets of eight adsorption systems. The number of experimental points, model parameters, and pressure range may have an impact on the type of results derived from the remaining statistical criteria. Tables 7 and 8 display the statistical error validity data for the isotherm models.

The adsorption kinetics of SAL and PRD onto the synthesized adsorbent were examined using several models, including pseudo-first-order, pseudo-second-order, mixed 1,2 order, Avrami, and intraparticle diffusion as illustrated in Table 9. All

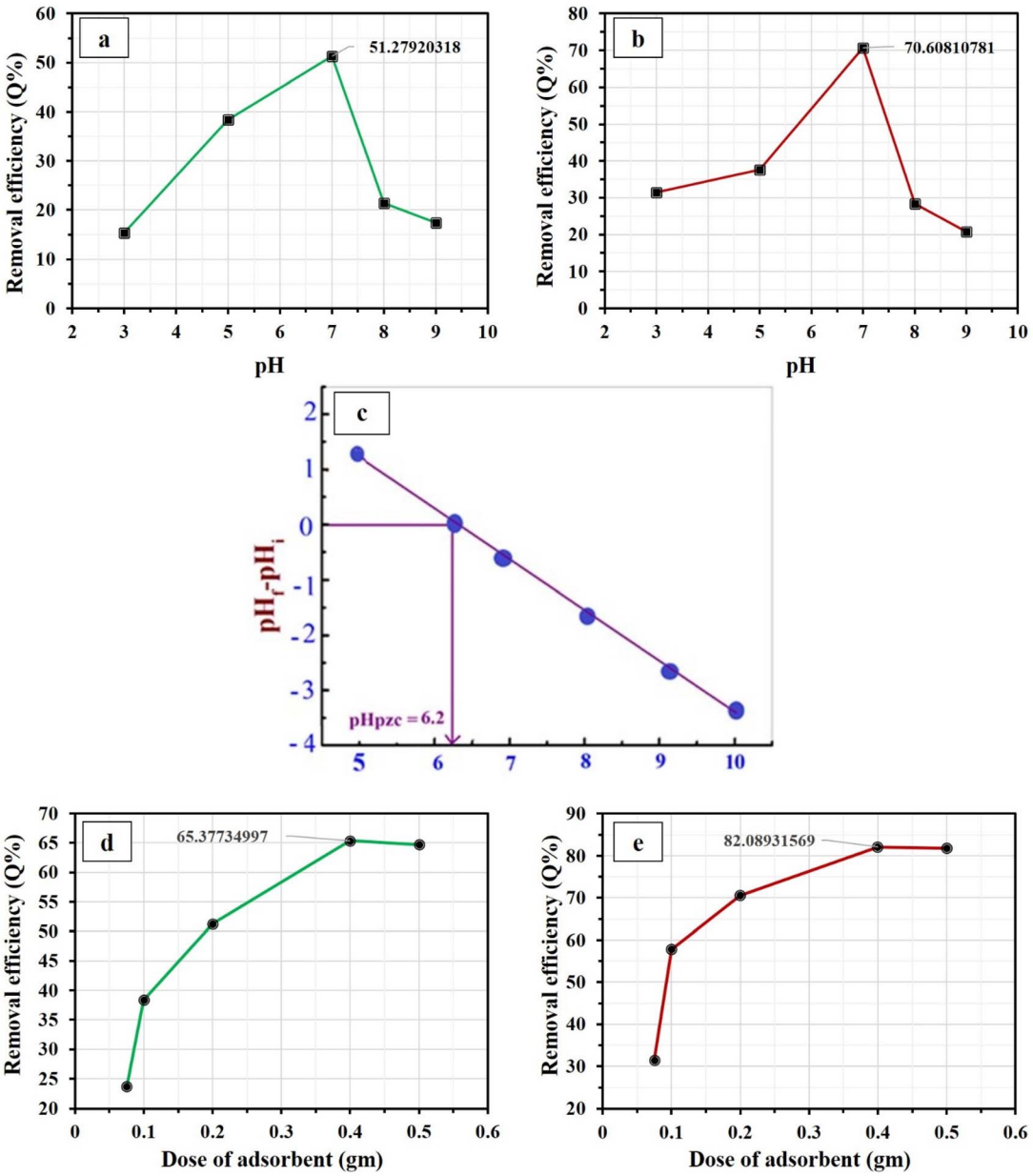

Fig. 8 (a and b) Effect of pH on the adsorption of (a) SAL and (b) PRD, while (c) PZC of OC/AC, (d and e) effect of dose of adsorbent on the removal efficiency of (d) SAL, (e) PRD.

models, except intraparticle diffusion, demonstrated excellent fits with high R^2 values, suggesting a complex adsorption process with multiple mechanisms. The pseudo-first-order model indicated a dependence on the number of unoccupied sites, while the pseudo-second-order model pointed to a chemisorption mechanism. The mixed 1,2 order model described both first- and second-order kinetics, and the Avrami model suggested a nucleation and growth process. Intraparticle diffusion contributed to the adsorption rate. The adsorption process, which involves physical and chemical interactions, surface adsorption, and intraparticle diffusion, was tracked by monitoring the removal efficiency of SAL and PRD, showing a rapid increase in the early stages due to the availability of vacant active sites, followed by equilibrium after 240 minutes. The pseudo-first-order, pseudo-second-order, mixed 1,2 order, and Avrami models best described the process with high R^2 values, while the intraparticle diffusion model provided a moderate fit with R^2 values of 0.68 and 0.70 for SAL and PRD, respectively, as illustrated in Fig. 11.

In the equations: q_t represents the adsorption capacity (mg g^{-1}) at time t (min), q_e represents the adsorption capacity (mg g^{-1}) at equilibrium, k_1 is the pseudo-first order rate constant (min^{-1}), k_2 is the pseudo-second order rate constant (min^{-1}), f_2 is the mixed 1,2 order coefficient (dimensionless), k

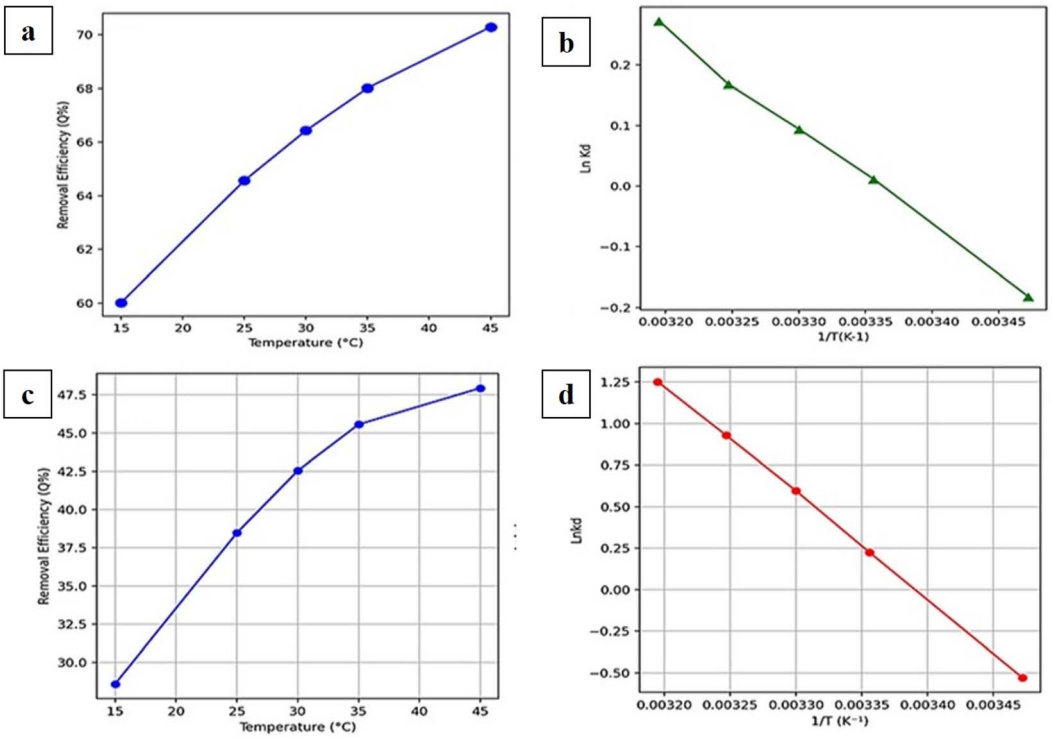

Fig. 9 (a) The effect of temperature on the removal efficiency to remove SAL; and (b) a plot of ln K_d against $1/T(K-1)$ for SAL, (c) The effect of temperature on the removal efficiency to remove PRD and (d) a plot of ln K_d against $1/T(K-1)$ for PRD.

is the adsorption rate constant (mg g^{-1} min^{-1}), k_{ip} is the measure of diffusion coefficient (mg g^{-1} $min^{-1/2}$), C_{ip} is the intraparticle diffusion constant (mg g^{-1}), k_{av} is the Avrami rate constant (min^{-1}), and n_{av} is the Avrami component (dimensionless).

3.4. Regeneration of adsorbent

Fig. 12a and b illustrates the performance of organoclay–activated carbon as an adsorbent for PRD and SAL across multiple regeneration cycles, showing the removal efficiency (effectiveness in extracting the drugs) in relation to the number of cycles. In the initial cycle, the adsorbent demonstrates high removal efficiency for both drugs, indicating strong adsorption capacity. However, as the cycles progress, the efficiency gradually declines, suggesting reduced effectiveness with repeated use. Without regeneration, ethanol consistently outperforms acetone and acetic acid as a desorbent for SAL, while acetone proves more effective than ethanol and acetic acid in releasing PRD. The decline in removal efficiency is most pronounced in the early cycles, particularly between the first and second, indicating a significant initial loss of capacity. Specifically, for acetic acid, the removal efficiency for PRD decreases from 97.83% to 89.78% and for SAL from 56.11% to 47.26%. With ethanol, PRD efficiency drops from 93.75% to 35.63% and SAL from 53.44% to 20.04%. For acetone, PRD removal decreases from 96.82% to 24.12% and SAL from 54.86% to 25.66%. These findings highlight the importance of developing effective regeneration strategies to sustain the performance of organoclay–activated carbon in drug removal applications.

3.5. Comparison with other adsorbents

Table 10 presents the maximum adsorption capacities of PRD and SAL for OC/AC, along with a comparison to other adsorbents. Given the q_{max} values of 888.7 mg g^{-1} for PRD and 731.64 mg g^{-1} for SAL, the OC/AC adsorbent is recommended as a promising, low-cost material for the removal of these pharmaceuticals. This material can be effectively utilized in water treatment facilities to address contamination caused by these pollutants.

3.6. Cost

Estimating the cost of the manufactured adsorbents is an essential part of performance study since cost-effective adsorbents offer significant advantages for real-world applications. It is possible to consider the organoclay–activated carbon cost estimate for this study to be acquisition-cost-free. According to Table 11, the equipment's energy costs which included a sonicator, a centrifuge, and a dryer were 0.12, 0.24, and 2.88 USD, respectively. With a yield of 3 g per batch, organoclay–activated carbon has an overall cost of about 1.08 USD per g. Compared to other water treatment adsorbents in previous reviews,[53,54] which were more expensive than the

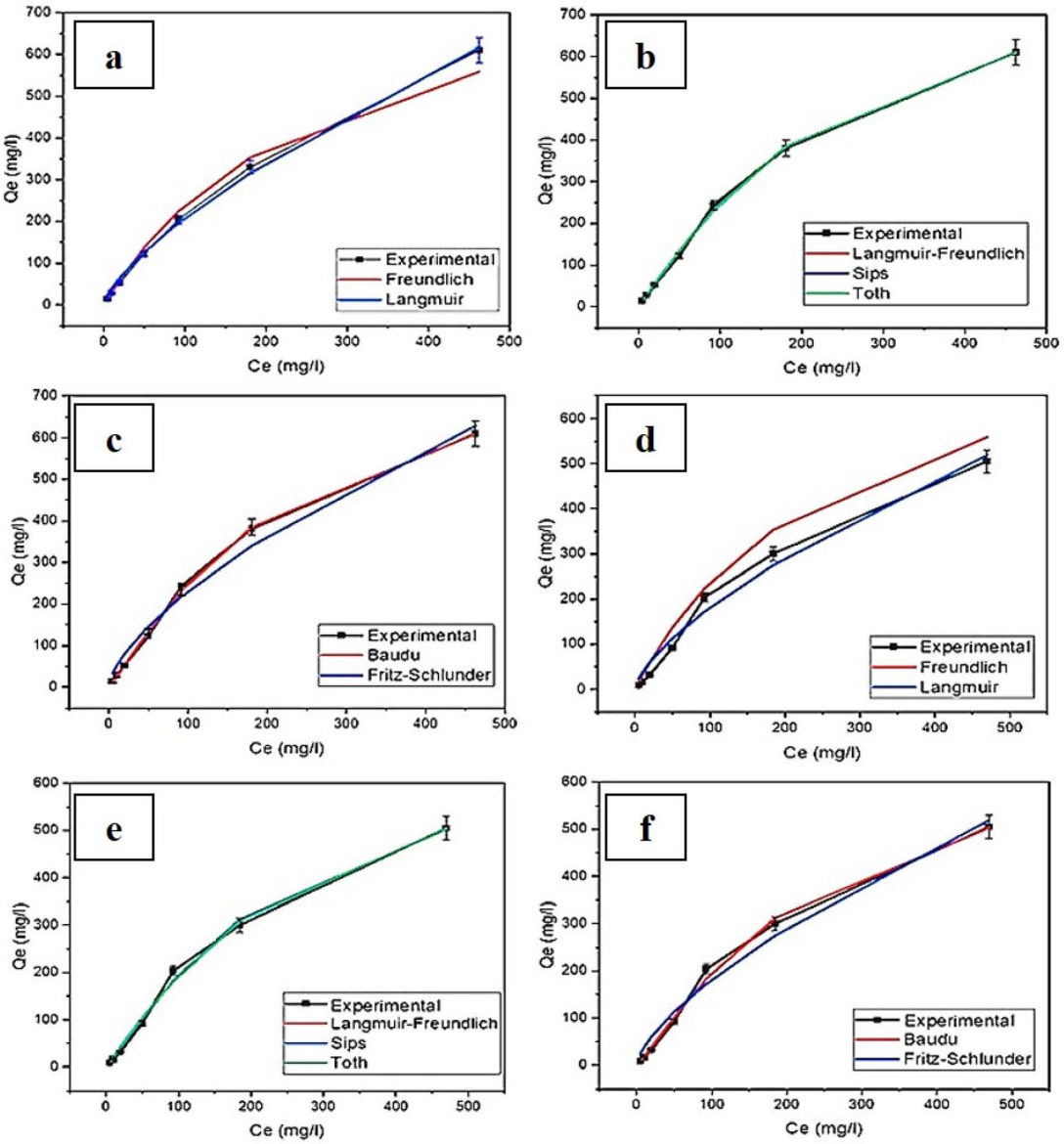

Fig. 10 Best fit isotherm model for (a–c) PRD and (d–f) SAL using the synthesized adsorbent.

manufactured organoclay–activated carbon, the cost analysis for this study demonstrated that organoclay–activated carbon was incredibly cost-effective.

3.7. Whiteness evaluation of the proposed method

Analytical methodologies' sustainability and eco-friendless must be assessed to evaluate how analytical technique or procedure can affect the environment and the eco-systems. However, sustainability is a broad term that includes affordability, efficiency, safety, waste reduction, and greenness. An analytical technique or procedure known as GAC reduces or eliminates solvents, chemicals, or other hazardous substances to the environment or public health. Sustainability cannot be fully examined using a single evaluation tool across all pertinent aspects.[55] GAC maintains quality standards while remaining quick and affordable.[56] Because of this, greenness, blueness, and whiteness evaluation for the proposed method in this work were evaluated using an integrated array of strategies that incorporates supportive approaches to enable a thorough evaluation from many perspectives.

3.7.1. The ComplexGAPI greenness tool. The color-coded pictogram used by the ComplexGAPI tool allows for an intensive visual evaluation of the greenness level at each step, with green being the most environmentally friendly and yellow to red being the least ecologically friendly.[57] The ComplexGAPI tool is reliable and commonly used partially quantitative criterion for evaluating greenness of analytical techniques or procedures. It improves the evaluation scope over the whole analytical process lifetime, including gathering the samples, storage, transport, preparing, preservation, and the analysis that follows. It

Table 6 The non-linear adsorption isotherm models for SAL and PRD using the synthesized adsorbent

Isotherm models	Expression	Adjustable model parameters	SAL	PRD
Two-parameters isotherm				
Langmuir	$q_e = \frac{q_{max} K_L C_e}{1 + K_L C_e}$	q_{max}	731.64	888.75
		K_L	0.004	0.0036
		R^2	0.99	0.99
Freundlich	$q_e = K_f C_e^{1/n_f}$	K_f	7.87	7.83
		$1/n_f$	0.68	0.71
		R^2	0.99	0.99
Three-parameters isotherm				
Langmuir–Freundlich	$q_e = \frac{q_{max}(K_{LF} C_e)^{\beta_{LF}}}{1 + (K_{LF} C_e)^{\beta_{LF}}}$	q_{max}	726.9	877.21
		K_{LF}	0.004	0.0044
		β_{LF}	1.17	1.14
		R^2	0.99	0.99
Sips	$q_e = \frac{q_{max} K_S C_e^{n_s}}{1 + K_S C_e^{n_s}}$	q_{max}	727	877.25
		K_S	0.001	0.0020
		n_s	1.17	1.14
		R^2	0.99	0.99
Redlich–Peterson		K_{RP}	2.23	2.85
		a_{RP}	0.001	0.00037
		β_{RP}	1.25	1.31
		R^2	0.99	0.99
Toth	$q_e = \frac{K_e C_e}{[1 + (K_T C_e)^{n_T}]^{1/n_T}}$	K_e	2.79	3.74
		K_T	0.001	0.0003
		n_T	1.25	1.34
		R^2	0.99	0.99
Four-parameters isotherm				
Baudu	$q_e = \frac{q_{max} b_o C_e^{1+X+Y}}{1 + b_o C_e^{1+X}}$	q_{max}	726.8	877.09
		b_o	0.001	0.002
		X	0.0001	0.00001
		Y	0.17	0.14
		R^2	0.99	0.99

Table 7 Summary of the determined error functions for the non-linear adsorption isotherm models for PRD adsorption onto OC/AC

	Lang	Fran	Lan–Fru	Toth	Sips	Baudu	Fritz–Schlunder
SSE/ERRSQ	3892.33	752.93	303.69	361.53	303.69	303.69	4805.95
X^2	11.33	16.3	3.02	2.19	3.02	3.03	66.65
R^2	0.99	0.99	0.99	0.99	0.99	0.99	0.99
Adjusted R^2	0.97	0.99	0.99	0.99	0.99	0.99	0.92
MAE	17.36	9.81	5.03	4.96	5.03	5.03	25.26
MAPE/ARE	10.13	21.23	7.67	3.92	7.66	7.67	42.67
RMSE	23.58	10.37	6.59	7.19	6.59	6.59	26.2
RMSE_2	27.9	12.27	8.71	9.51	8.71	10.06	40.02
NRMSE	0.23	0.1	0.06	0.06	0.06	0.06	0.23
HYBRID	14.18	29.72	13.42	6.85	13.41	17.9	99.57
HYBRID_2	226.61	326	75.62	54.67	75.59	100.86	2221.58
HYBRID_3	11.33	16.3	3.02	2.19	3.02	3.03	66.65
MPSD	12.36	37.61	14.69	6.66	14.68	16.97	90.57
MPSD_2	0.08	0.71	0.09	0.02	0.09	0.09	2.46
SAE/EABS	121.53	68.68	35.21	34.71	35.2	35.22	176.79
RMS	10.45	31.79	11.1	5.04	11.1	11.11	59.29
NSD	0.1	0.32	0.11	0.05	0.11	0.11	0.59
ARE_2	1.09	10.1	1.23	0.25	1.23	1.23	35.15
ARE_3	3.95	12.01	4.2	1.9	4.19	4.2	22.41

Table 8 Summary of the determined error functions for the non-linear adsorption isotherm models for SAL adsorption onto OC/AC

	Lang	Fran	Lan–Fru	Toth	Sips	Baudu	Fritz–Schlunder
SSE/ERRSQ	2422.29	3735.29	707.76	891.89	707.76	707.75	3735.29
X^2	36.88	91.33	4.89	11.17	4.89	4.88	91.35
R^2	0.99	0.98	0.99	0.99	0.99	0.99	0.98
Adjusted R^2	0.97	0.95	0.99	0.99	0.99	0.98	0.91
MAE	16.03	22.28	7.51	9.08	7.51	7.51	22.28
MAPE/ARE	35.07	63.4	8.59	18.25	8.59	8.59	63.41
RMSE	18.6	23.1	10.06	11.29	10.06	10.06	23.1
RMSE_2	22.01	27.33	13.3	14.93	13.3	15.36	35.29
NRMSE	0.21	0.26	0.11	0.13	0.11	0.11	0.26
HYBRID	49.09	88.76	15.03	31.93	15.04	20.04	147.95
HYBRID_2	737.69	1826.55	122.13	279.36	122.24	162.83	3045.02
HYBRID_3	36.88	91.33	4.89	11.17	4.89	4.88	91.35
MPSD	54.18	106.22	13.38	30.42	13.39	15.45	137.15
MPSD_2	1.47	5.64	0.07	0.37	0.07	0.07	5.64
SAE/EABS	112.18	155.98	52.55	63.58	52.56	52.55	155.98
RMS	45.79	89.77	10.11	23	10.12	10.11	89.79
NSD	0.46	0.9	0.1	0.23	0.1	0.1	0.9
ARE_2	20.97	80.59	1.02	5.29	1.02	1.02	80.62
ARE_3	17.31	33.93	3.82	8.69	3.83	3.82	33.94

Table 9 Represents the kinetic models' parameters

Kinetic models	Equation	Parameters	SAL	PRD
Pseudo first order	$q_t = q_e(1 - e^{-k_1 t})$	k_1	0.013	0.012
		q_e	66.06	81.13
		R^2	0.99	0.99
Pseudo second order	$q_t = {q_e}^2 \frac{k_2 t}{1 + q_e k_2 t}$	k_2	0.0003	0.0002
		q_e	72.15	88.39
		R^2	0.99	0.99
Mixed 1,2 orders	$q_t = q_e \frac{(1 - \exp(-kt))}{1 - f_2 \exp(-kt)}$	k	0.014	0.0088
		q_e	66.06	81.69
		f_2	0	0.39
		R^2	0.99	0.99
Avrami	$q_t = q_e[1 - \exp(-k_{av}t)^{n_{av}}]$	q_e	66.06	81.13
		k_{av}	0.24	0.225
		n_{av}	0.057	0.053
		R^2	0.99	0.99
Intraparticle diffusion	$q_t = k_{ip}\sqrt{t} + C_{ip}$	k_{ip}	1.80	2.16
		C_{ip}	18.79	23.67
		R^2	0.68	0.70

performs this by improving the current GAPI index and adding new parameters based on the CHEM21 recommendations. In contrast to the initial GAPI technique, this tool for assessment better includes the 12 GAC principles. A substantial amount of information about the specifics and related aspects of the process must be obtained, comprehended, and included for the assessment to be valid. However, ComplexGAPI's overall findings can be attained by combining GAPI with additional analysis approaches. We can see from Fig. 13a, how sustainable our suggested approach is, in which the *E*-factor, which refers to an extremely remarkable one, denotes less waste production (1.20*E*, 00), and leads to improved sustainability and a favorable effect on the environment.

3.7.2. The AGREEprep greenness tool. To evaluate the stage of preparing the samples, an innovative greenness measuring method called AGREEprep was developed in 2022 as a modification to the old AGREE gadget. A total of ten variables contribute to the overall evaluation score. The factors score was score on a scale from 0.00 to 1.00 and weigh them differently. Certain assessments incorporate the following categories: solvents, chemicals, reagents, materials, waste, energy, and results.[58] Fig. 13b shows that the recommended method is environmentally eco-friendly (0.91), with exceptional greenness as a sustainable analytical technique.

3.7.3. The BAGI blueness tool. The recently developed BAGI assesses an analytical method's "blueness," or its practicality and application.[59] Although ComplexGAPI and AGREEprep are tools that mostly assess an analytical method's greenness, the ten useful criteria, such as evaluation type, total number of analytes, equipment demands, sample efficiency,

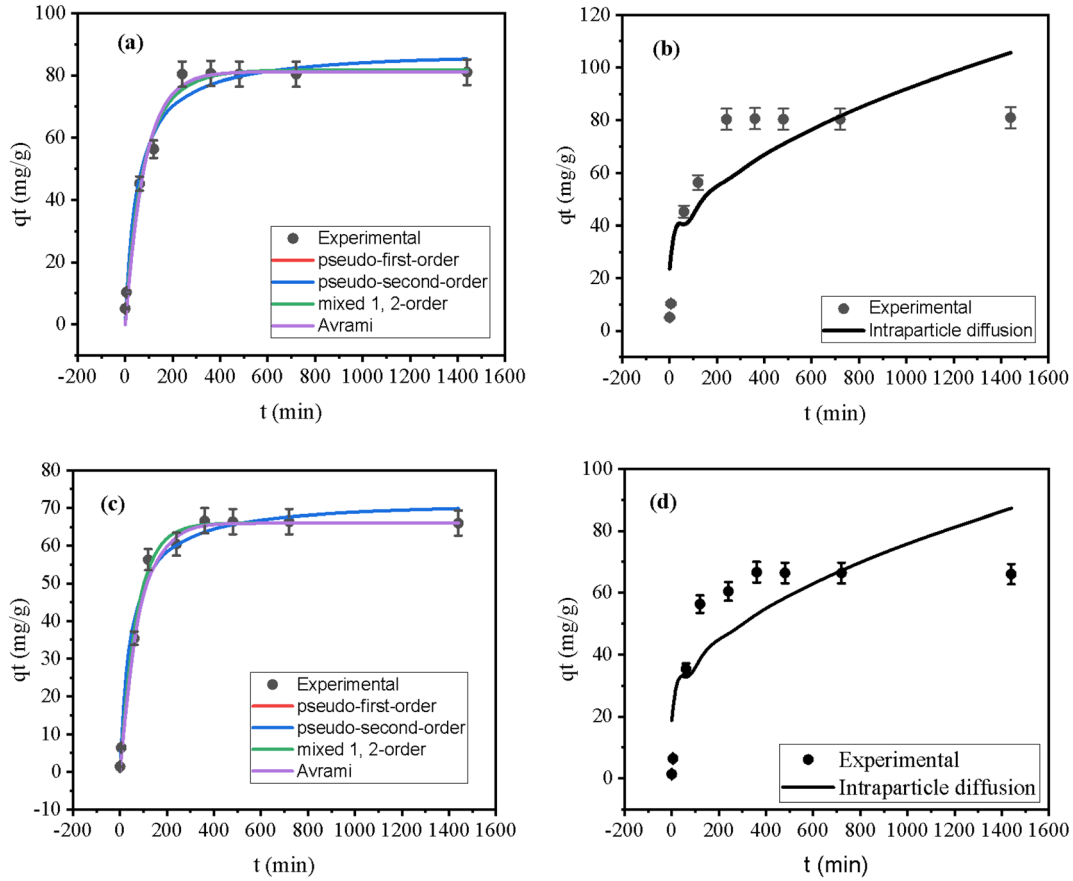

Fig. 11 Kinetic models fitting for (a and b) PRD and (c and d) SAL adsorption onto using organoclay–activated carbon adsorbents.

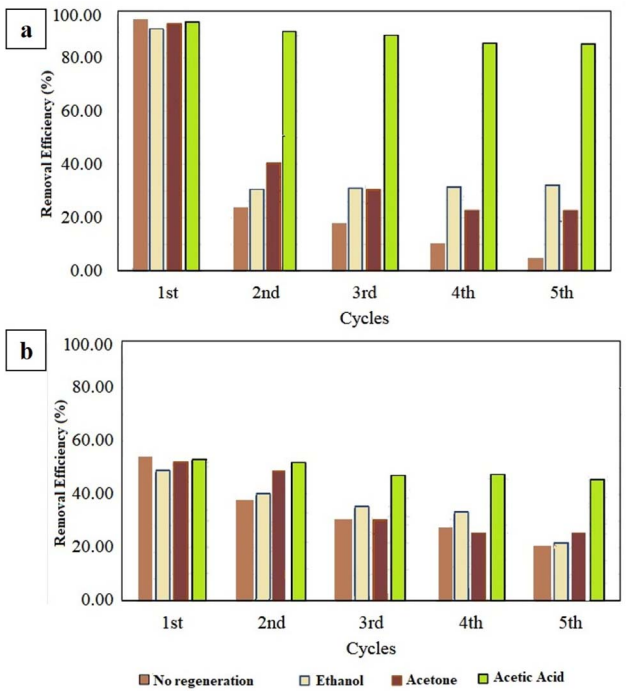

Fig. 12 Performance of various regeneration materials of organoclay–activated carbon for (a) PRD removal, (b) SAL.

prepared sample needs, analysis percentage, reagents/materials used, preliminary concentration needs, automation perspective, and sample volume, can be quantitatively evaluated for blueness using the BAGI tool. The approximate mean of these scores is used to calculate the composite BAGI index. Each of these characteristics is rated from 1 (worst) to 10 (best). To assess the blueness of our suggested method, we used the BAGI tool in our study. As shown in Fig. 14a, our method achieved remarkable BAGI rankings of 90.0, demonstrating its exceptional practical applicability, high production capabilities, automation potential, and extremely low operating costs.

3.7.4. The RGB12 whiteness tool. The RGB12 approach consists of 12 different algorithms that are grouped into three categories: red, green, and blue. Each group of algorithms covers important sustainability-related aspects.[60] The G1–G4 green group concentrates on critical factors such as poisoning, extra reagent and waste use, energy use, and possible effects on humans, animals, and manipulated species. Validation criteria, such as the method's applicability, LOD and LOQ, precision, and accuracy, are evaluated by the red group (R1–R4). The blue group (B1–B4) assesses elements of cost-effectiveness, convenience, practicality concerns, and budgetary requirements. The RGB12 algorithm is used to combine the scores for each of the three-color groups to

Table 10 q_{max} values gained for various materials for PRD and SAL uptake

Pollutant	Adsorbent	q_{max} (mg g^{-1})	Ref.
PRD	Montmorillonite clay	18.04	45
PRD	Graphene oxide	22.94	46
PRD	Mesoporous materials	9.259	47
PRD	Nanobiochar-enriched-diamine	21.93	48
PRD	Poly aniline-*co*-pyrrole	238.8	49
PRD	OC/AC	888.7	Current work
SAL	Electronegative silanized β-cyclodextrin	159.6	50
SAL	Cyclodextrin-based adsorbents	140.2	51
SAL	Anionic cellulose nanofibrils	196.0	52
SAL	OC/AC	731.64	Current work

Table 11 Cost estimation of organoclay–activated carbon preparation

Equipment	Time (h)	Max. power (kW)	Unit cost of power	Cost
Sonicator	30 min = 0.5 h	1	0.24	0.12
Centrifuge	1	1	0.24	0.24
Dryer	12	1	0.24	2.88
Total yield cost = 3.24 USD for 3 g			Total yield cost = 1.08 USD per g	

estimate the whiteness value, which indicates how closely the procedure adheres to the guidelines of White Analytical Chemistry (WAC). Using the RGB 12 algorithm, an extensive study is conducted to quantitatively assess the overall sustainability level of our analytical procedures, and to evaluate the whiteness profile of our suggested techniques. Fig. 14b, demonstrates that the recommended procedures for our proposed method, resulted in good whiteness value of 89.0. This evaluation highlights the enhanced reliability, performance, and economic feasibility of our proposed approach.[61–68]

4 Study limitations and future research plan

Although this study demonstrated the effectiveness of the developed RP-HPLC method and organoclay–activated carbon composite adsorbent, several limitations should be acknowledged. First, the study focused on only two pharmaceutical compounds, and the method's applicability to a broader range of pharmaceuticals remains to be explored. Additionally, while the adsorbent showed promising results in laboratory conditions, real-world water matrices with complex chemical compositions may present challenges in adsorption efficiency and stability. Further research is needed to investigate the performance of this composite adsorbent in more diverse environmental conditions, including varying water types and concentrations of interfering substances. Additionally, the regeneration potential of the adsorbent should be studied in greater depth to assess its long-term sustainability in large-scale applications. Future studies could also explore the integration of this method with other water treatment techniques to optimize removal efficiency and reduce environmental impact.

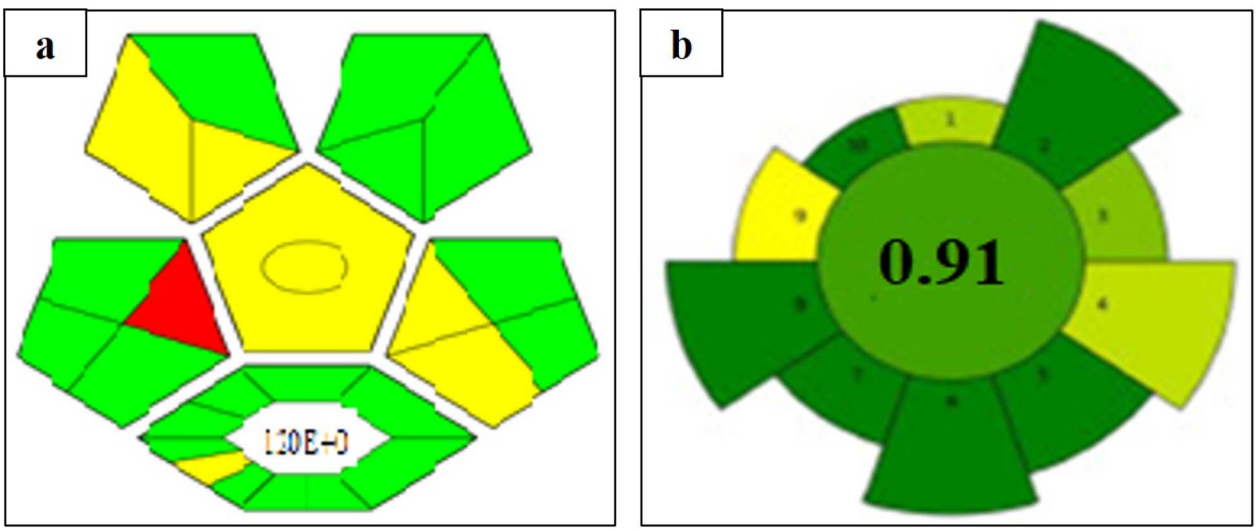

Fig. 13 The greenness evaluation tools of the proposed method: (a) the ComplexGAPI greenness tool and (b) the AGREEprep greenness tool.

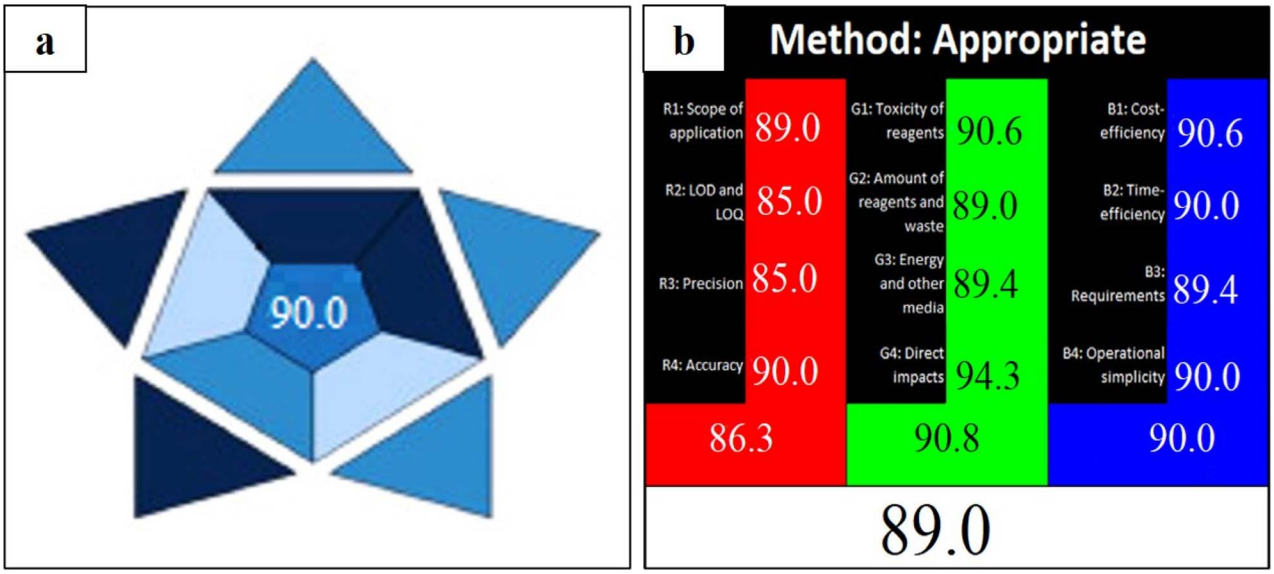

Fig. 14 The blueness and whiteness evaluation tools of the proposed method: (a) the BAGI blueness tool and (b) the RGB12 whiteness tool.

Moreover, investigating the environmental fate and toxicity of SAL and PRD after treatment will contribute to understanding the long-term benefits of such water treatment methods.

5 Conclusion

This study successfully developed a reliable RP-HPLC method for quantifying salbutamol sulfate (SAL) and prednisolone (PRD) in pharmaceutical and environmental samples, demonstrating high precision, accuracy, and reliability for routine quality control and environmental monitoring. Additionally, an organoclay–activated carbon composite adsorbent was engineered to efficiently remove SAL and PRD from water, with optimal conditions at pH 7, 45 °C, and a 0.4 g dose, achieving maximum adsorption capacities of 731.64 mg g^{-1} for SAL and 888.75 mg g^{-1} for PRD. The Langmuir model was identified as the most suitable representation of the isotherm data at 25 °C, as evidenced by the lowest recorded χ^2 values. As a result, the removal of both PRD and SAL can be attributed to the formation of a monolayer of PRD and SAL molecules, facilitated by the similar functional groups present on the surface of the synthesized OC/AC adsorbent. The adsorption process was endothermic and spontaneous, supporting its potential for large-scale applications. This cost-effective adsorbent also proved environmentally friendly, as confirmed by sustainability assessments using ComplexGAPI, BAGI, and RGB 12 algorithms. Overall, the combined RP-HPLC method and organoclay–activated carbon adsorbent provide a scalable and sustainable solution for detecting and removing pharmaceutical pollutants, contributing to the protection of aquatic ecosystems and biodiversity.

Data availability

The authors declare that the data supporting the findings of this study are available within the article.

Conflicts of interest

The authors declare no competing interests.

Acknowledgements

The authors acknowledge Princess Nourah bint Abdulrahman University Researchers Supporting Project number (PNURSP2025R400), Princess Nourah bint Abdulrahman University, Riyadh, Saudi Arabia.

References

1 K. Samal, S. Mahapatra and M. H. Ali, Pharmaceutical Wastewater as Emerging Contaminants (EC): Treatment Technologies, Impact on Environment and Human Health, *Energy Nexus*, 2022, **6**, 100076.
2 T. Aus der Beek, F. Weber, A. Bergmann, S. Hickmann, I. Ebert, A. Hein and A. Küster, Pharmaceuticals in the Environment—Global Occurrences and Perspectives, *Environ. Toxicol. Chem.*, 2016, **35**, 823–835.
3 W. C. Li, Occurrence, Sources, and Fate of Pharmaceuticals in Aquatic Environment and Soil, *Environ. Pollut.*, 2014, **187**, 193–201.
4 U. Armaya'u, M. M. Ariffin, S. H. Loh, W. M. A. W. Mohd Khalik and H. M. Yusoff, β-Agonist in the Environmental Waters: A Review on Threats and Determination Methods, *Green Chem. Lett. Rev.*, 2022, **15**, 233–252.
5 M. D. Hernando, M. Mezcua, A. R. Fernández-Alba and D. Barceló, Environmental Risk Assessment of Pharmaceutical Residues in Wastewater Effluents, Surface Waters and Sediments, *Talanta*, 2006, **69**, 334–342.
6 A. R. Cole and B. W. Brooks, Global Occurrence of Synthetic Glucocorticoids and Glucocorticoid Receptor Agonistic Activity, and Aquatic Hazards in Effluent Discharges and Freshwater Systems, *Environ. Pollut.*, 2023, **329**, 121638.

7 K. Fent, A. A. Weston and D. Caminada, Ecotoxicology of Human Pharmaceuticals, *Aquat. Toxicol.*, 2006, **76**, 122–159.
8 M. DellaGreca, A. Fiorentino, M. Isidori, M. Lavorgna, L. Previtera, M. Rubino and F. Temussi, Toxicity of Prednisolone, Dexamethasone and Their Photochemical Derivatives on Aquatic Organisms, *Chemosphere*, 2004, **54**, 629–637.
9 N. Bal, A. Kumar, J. Du and D. Nugegoda, Multigenerational Effects of Two Glucocorticoids (Prednisolone and Dexamethasone) on Life-History Parameters of Crustacean Ceriodaphnia Dubia (Cladocera), *Environ. Pollut.*, 2017, **225**, 569–578.
10 J. O. Eniola, R. Kumar, M. A. Barakat and J. Rashid, A Review on Conventional and Advanced Hybrid Technologies for Pharmaceutical Wastewater Treatment, *J. Cleaner Prod.*, 2022, **356**, 131826.
11 F. Mansouri, K. Chouchene, N. Roche and M. Ksibi, Removal of Pharmaceuticals from Water by Adsorption and Advanced Oxidation Processes: State of the Art and Trends, *Appl. Sci.*, 2021, **11**, 6659.
12 P. Verlicchi, M. Al Aukidy and E. Zambello, Occurrence of Pharmaceutical Compounds in Urban Wastewater: Removal, Mass Load and Environmental Risk after a Secondary Treatment—a Review, *Sci. Total Environ.*, 2012, **429**, 123–155.
13 I. Sevgili, Ö. F. Dilmaç and B. Şimşek, An Environmentally Sustainable Way for Effective Water Purification by Adsorptive Red Mud Cementitious Composite Cubes Modified with Bentonite and Activated Carbon, *Sep. Purif. Technol.*, 2021, **274**, 119115.
14 J.-H. Park, H.-J. Shin, M. H. Kim, J.-S. Kim, N. Kang, J.-Y. Lee, K.-T. Kim, J. I. Lee and D.-D. Kim, Application of Montmorillonite in Bentonite as a Pharmaceutical Excipient in Drug Delivery Systems, *J. Pharm. Invest.*, 2016, **46**, 363–375.
15 R. Leyva-Ramos, A. Jacobo-Azuara and J. I. Martínez-Costa, Organoclays. Fundamentals and Applications for Removing Toxic Pollutants from Water Solution, *Porous Materials Theory and Its Application for Environmental Remediation: Theory and Its Application for Environmental Remediation*, 2021, pp. 341–363.
16 G. Lagaly, Clay-Organic Interactions, *Philos. Trans. R. Soc., A*, 1984, **311**, 315–332.
17 G. Lagaly, M. Ogawa and I. Dékány, Clay Mineral Organic Interactions, *Dev. Clay Sci.*, 2006, **1**, 309–377.
18 K. Nadafi, M. Tayefeh Rafi and A. Gholampour, Application of Chitosan in Water and Wastewater Treatment, in *Proceedings of the the 8th National Environmental Health Conference*, 2005, in Persian.
19 M. Patel, R. Kumar, K. Kishor, T. Mlsna, C. U. Pittman and D. Mohan, Pharmaceuticals of Emerging Concern in Aquatic Systems: Chemistry, Occurrence, Effects, and Removal Methods, *Chem. Rev.*, 2019, **119**, 3510–3673, DOI: 10.1021/acs.chemrev.8b00299.
20 J. Wang, J. Shen, D. Ye, X. Yan, Y. Zhang, W. Yang, X. Li, J. Wang, L. Zhang and L. Pan, Disinfection Technology of Hospital Wastes and Wastewater: Suggestions for Disinfection Strategy during Coronavirus Disease 2019 (COVID-19) Pandemic in China, *Environ. Pollut.*, 2020, **262**, 114665, DOI: 10.1016/j.envpol.2020.114665.
21 H. I. Abdel-Shafy and M. S. Mohamed-Mansour, Issue of Pharmaceutical Compounds in Water and Wastewater: Sources, Impact and Elimination, *Egypt. J. Chem.*, 2013, **56**, 449–471.
22 ICHEW Group, ICH Q2 (R1) Validation of Analytical Procedure: Text and Methodology: ICH Harmonized Tripartite Guideline, in *Proceedings of the International Conference on Harmonization of Technical Requirements for Registration of Pharmaceuticals for Human Use*, Geneva, 2005.
23 K. Huynh-Ba and R. C. Moreton, Development of United States Pharmacopeia-National Formulary (USP–NF) Monographs and General Chapters, in *Specification of Drug Substances and Products*, Elsevier, 2025, pp. 185–204.
24 H. Xue, X. Wang, Q. Xu, F. Dhaouadi, L. Sellaoui, M. K. Seliem, A. B. Lamine, H. Belmabrouk, A. Bajahzar and A. Bonilla-Petriciolet, Adsorption of Methylene Blue from Aqueous Solution on Activated Carbons and Composite Prepared from an Agricultural Waste Biomass: A Comparative Study by Experimental and Advanced Modeling Analysis, *Chem. Eng. J.*, 2022, **430**, 132801.
25 M. A. Alaa, K. Yusoh and S. F. Hasany, Synthesis and Characterization of Polyurethane–Organoclay Nanocomposites Based on Renewable Castor Oil Polyols, *Polym. Bull.*, 2015, **72**, 1–17.
26 N. Mojoudi, N. Mirghaffari, M. Soleimani, H. Shariatmadari, C. Belver and J. Bedia, Phenol Adsorption on High Microporous Activated Carbons Prepared from Oily Sludge: Equilibrium, Kinetic and Thermodynamic Studies, *Sci. Rep.*, 2019, **9**, 19352.
27 H. Zaitan, D. Bianchi, O. Achak and T. Chafik, A Comparative Study of the Adsorption and Desorption of O-Xylene onto Bentonite Clay and Alumina, *J. Hazard. Mater.*, 2008, **153**, 852–859.
28 H. S. Ramadan, M. Mobarak, E. C. Lima, A. Bonilla-Petriciolet, Z. Li and M. K. Seliem, Cr (VI) Adsorption onto a New Composite Prepared from Medium Black Clay and Pomegranate Peel Extract: Experiments and Physicochemical Interpretations, *J. Environ. Chem. Eng.*, 2021, **9**, 105352.
29 H. N. Tran, S.-J. You and H.-P. Chao, Insight into Adsorption Mechanism of Cationic Dye onto Agricultural Residues-Derived Hydrochars: Negligible Role of π-π Interaction, *Korean J. Chem. Eng.*, 2017, **34**, 1708–1720.
30 O. Duman, T. G. Polat, C. Ö. Diker and S. Tunç, Agar/κ-Carrageenan Composite Hydrogel Adsorbent for the Removal of Methylene Blue from Water, *Int. J. Biol. Macromol.*, 2020, **160**, 823–835.
31 P. Szabová, D. Varjúová, M. Kováčová, J. Prousek and I. Bodík, What Is the Effect of Changing pH on Pharmaceuticals' Sorption?, *Pol. J. Environ. Stud.*, 2022, **31**(2), 1805–1812.
32 A. C. Hari, R. A. Paruchuri, D. A. Sabatini and T. C. G. Kibbey, Effects of PH and Cationic and Nonionic Surfactants on the

Adsorption of Pharmaceuticals to a Natural Aquifer Material, *Environ. Sci. Technol.*, 2005, **39**, 2592–2598.
33 R. Imboden and G. Imanidis, Effect of the Amphoteric Properties of Salbutamol on Its Release Rate through a Polypropylene Control Membrane, *Eur. J. Pharm. Biopharm.*, 1999, **47**, 161–167.
34 M. J. O'Neil, A. Smith and P. E. Heckelman, *The Merck Index—An Encyclopedia of Chemicals, Drugs, and Biologicals*, Merck and Co. Inc., Whitehouse Station, NJ, USA, 2006, p. 1204.
35 A. Davis and S. E. Ward, *The Handbook of Medicinal Chemistry: Principles and Practice*, Royal Society of Chemistry, 2014, ISBN 1849736251.
36 T. Tatarchuk, L. Soltys and W. Macyk, Magnetic Adsorbents for Removal of Pharmaceuticals: A Review of Adsorption Properties, *J. Mol. Liq.*, 2023, **384**, 122174.
37 O. Fraiha, N. Hadoudi, N. Zaki, A. Salhi, H. Amhamdi, E. H. Akichouh, F. Mourabit and M. Ahari, Comprehensive Review on the Adsorption of Pharmaceutical Products from Wastewater by Clay Materials, *Desalin. Water Treat.*, 2024, **317**, 100114, DOI: **10.1016/j.dwt.2024.100114**.
38 D. T. Bankole, A. P. Oluyori and A. A. Inyinbor, The Removal of Pharmaceutical Pollutants from Aqueous Solution by Agro-Waste, *Arabian J. Chem.*, 2023, **16**, 104699, DOI: **10.1016/j.arabjc.2023.104699**.
39 M. Kryuchkova, S. Batasheva, F. Akhatova, V. Babaev, D. Buzyurova, A. Vikulina, D. Volodkin, R. Fakhrullin and E. Rozhina, Pharmaceuticals Removal by Adsorption with Montmorillonite Nanoclay, *Int. J. Mol. Sci.*, 2021, **22**, 9670, DOI: **10.3390/ijms22189670**.
40 J. Maszkowska, M. Wagil, K. Mioduszewska, J. Kumirska, P. Stepnowski and A. Białk-Bielińska, Thermodynamic Studies for Adsorption of Ionizable Pharmaceuticals onto Soil, *Chemosphere*, 2014, **111**, 568–574.
41 I. Allaoui, M. El Mourabit, B. Arfoy, M. Hadri, A. Barhoun and K. Draoui, Adsorption Equilibrium, Kinetic, and Thermodynamic Studies on the Removal of Paracetamol from Wastewater Using Natural and HDTMA-Modified Clay, *Desalin. Water Treat.*, 2024, **318**, 100345, DOI: **10.1016/j.dwt.2024.100345**.
42 L. A. Al-Khateeb, S. Almotiry and M. A. Salam, Adsorption of Pharmaceutical Pollutants onto Graphene Nanoplatelets, *Chem. Eng. J.*, 2014, **248**, 191–199.
43 T. De Oliveira, M. Boussafir, L. Fougère, E. Destandau, Y. Sugahara and R. Guégan, Use of a Clay Mineral and Its Nonionic and Cationic Organoclay Derivatives for the Removal of Pharmaceuticals from Rural Wastewater Effluents, *Chemosphere*, 2020, **259**, 127480.
44 I. Langmuir, The Adsorption of Gases on Plane Surfaces of Glass, Mica and Platinum, *J. Am. Chem. Soc.*, 1918, **40**, 1361–1403, DOI: **10.1021/ja02242a004**.
45 J. C. Zanette, M. T. Veit, G. C. Gonçalves, S. M. Palácio, F. R. Scremin, A. S. Torquato and M. R. S. A. Vieira, A Study on the Removal of Prednisone from Aqueous Solutions by Adsorption onto a Vegetal Activated Carbon, *Water Sci. Technol.*, 2018, **78**, 2328–2337.
46 S. Bhattacharyya, P. Banerjee, S. Bhattacharya, R. K. S. Rathour, S. K. Majumder, P. Das and S. Datta, Comparative Assessment on the Removal of Ranitidine and Prednisolone Present in Solution Using Graphene Oxide (GO) Nanoplatelets, *Desalin. Water Treat.*, 2018, **132**, 287–296.
47 T. M. Albayati and A. J. Abd Alkadir, Synthesis and Characterization of Mesoporous Materials as a Carrier and Release of Prednisolone in Drug Delivery System, *J. Drug Delivery Sci. Technol.*, 2019, **53**, 101176.
48 M. E. Mahmoud, A. M. El-Ghanam and S. R. Saad, Sequential Removal of Chromium (VI) and Prednisolone by Nanobiochar-Enriched-Diamine Derivative, *Biomass Convers. Biorefin.*, 2024, **14**, 7011–7030.
49 T. A. Nascimento, B. C. Pires, F. V. A. Dutra, M. M. C. Borges and K. B. Borges, Poly (Aniline-co-pyrrole) as Adsorbent for Removal of Pharmaceuticals: Preparation, Characterization, Kinetics, Isotherms and Application on Sample Preparation, *ChemistrySelect*, 2024, **9**, e202305101.
50 C. Duan, J. Wang, Q. Liu, Y. Zhou and Y. Zhou, Efficient Removal of Salbutamol and Atenolol by an Electronegative Silanized β-Cyclodextrin Adsorbent, *Sep. Purif. Technol.*, 2022, **282**, 120013.
51 S. E. Z. Syeda, D. Nowacka, M. S. Khan and A. M. Skwierawska, Recent Advancements in Cyclodextrin-Based Adsorbents for the Removal of Hazardous Pollutants from Waters, *Polymers*, 2022, **14**, 2341.
52 T. Selkälä, T. Suopajärvi, J. A. Sirviö, T. Luukkonen, G. S. Lorite, S. Kalliola, M. Sillanpää and H. Liimatainen, Rapid Uptake of Pharmaceutical Salbutamol from Aqueous Solutions with Anionic Cellulose Nanofibrils: The Importance of PH and Colloidal Stability in the Interaction with Ionizable Pollutants, *Chem. Eng. J.*, 2018, **350**, 378–385.
53 A. Syafiuddin, S. Salmiati, T. Hadibarata, M. R. Salim, A. B. H. Kueh and S. Suhartono, Removal of Silver Nanoparticles from Water Environment: Experimental, Mathematical Formulation, and Cost Analysis, *Water, Air, Soil Pollut.*, 2019, **230**, 1–15.
54 R. Abdelazeem, H. A. Younes, Z. E. Eldin, A. A. Allam, H. A. Rudayni, S. I. Othman, A. A. Farghali, H. M. Mahmoud and R. A. Mahmoud, Selective, Efficient, Facile, and Reusable Natural Clay/Metal Organic Framework as a Promising Adsorbent for the Removal of Drug Residue and Heavy Metal Ions, *Colloids Interfaces*, 2024, **8**, 50.
55 S. M. Mahgoub, M. R. Mahmoud, A. Y. Binsaleh, M. A. Almalki, M. A. Mohamed and H. F. Nassar, Analytical Assessment of a Novel RP-HPLC Method for the Concurrent Quantification of Selected Pharmaceutical Drugs Levodopa and Carbidopa Using Eight Greenness Metrics Comparing to the Lean Six Sigma Approach, *Sustainable Chem. Pharm.*, 2023, **36**, 101291.
56 H. M. Nassef, H. A. Ahmed, A. H. Bashal, M. A. El-Atawy, T. Y. A. Alanazi, S. M. Mahgoub and M. A. Mohamed, A Novel Six Sigma Approach and Eco-Friendly RP-HPLC Technique for Determination of Pimavanserin and Its

Degraded Products: Application of Box–Behnken Design, *Rev. Anal. Chem.*, 2024, **43**, 20230073.

57 J. Płotka-Wasylka and W. Wojnowski, Complementary Green Analytical Procedure Index (ComplexGAPI) and Software, *Green Chem.*, 2021, **23**, 8657–8665, DOI: **10.1039/d1gc02318g**.

58 T. Y. A. Alanazi, M. A. Almalki, M. A. Mohamed and H. F. Nassar, Five Greenness Assessments of Novel RP-UPLC and MCR Methods for Concurrent Determination of Selected Pharmaceutical Drugs in Comparison with the Lean Six Sigma Approach, *Microchem. J.*, 2023, **194**, 109359.

59 N. Manousi, W. Wojnowski, J. Płotka-Wasylka and V. Samanidou, Blue Applicability Grade Index (BAGI) and Software: A New Tool for the Evaluation of Method Practicality, *Green Chem.*, 2023, **25**, 7598–7604, DOI: **10.1039/d3gc02347h**.

60 P. M. Nowak, R. Wietecha-Posłuszny and J. Pawliszyn, White Analytical Chemistry: An Approach to Reconcile the Principles of Green Analytical Chemistry and Functionality, *TrAC, Trends Anal. Chem.*, 2021, **138**, 116223.

61 M. A. M. Momin, M. F. Hossain, A. A. Begum, J. Roy and S. M. Anisuzzaman, Development and Validation of Stability Indicating Assay Method of Salbutamol Sulphate Metered Dose Inhaler by HPLC, *Int. J. Pharm. Phytopharm. Res.*, 2013, **2**, 439–448.

62 G. Murtaza, M. Ahmad, M. A. Madni and M. W. Asghar, A New Reverse Phase HPLC Method with Fluorescent Detection for the Determination of Salbutamol Sulfate in Human Plasma, *Bull. Chem. Soc. Ethiop.*, 2009, **23**, 1–8.

63 F. M. Abdoon and S. Y. Yahyaa, Validated Spectrophotometric Approach for Determination of Salbutamol Sulfate in Pure and Pharmaceutical Dosage Forms Using Oxidative Coupling Reaction, *J. King Saud Univ., Sci.*, 2020, **32**, 709–715.

64 G. R. Gadekar, S. S. Patil, R. R. Shah and D. S. Ghodke, Development and Validation of a Simple UV Spectrophotometric Method for the Estimation of Salbutamol Sulphate from Pharmaceutical Formulations, *Int. J. Curr. Pharm. Res.*, 2019, **11**, 72–75.

65 N. Abdullah, F. Karamat, S. Qamar, M. Abbas, A. Khan and N. Ullah, Development and Validation of RP-HPLC Method for Simultaneous Quantification of Sulfacetamide Sodium and Prednisolone Sodium Phosphate, *Acta Pol. Pharm.*, 2019, **76**, 37–47.

66 A. S. Ali and A. S. Rasheed, Application of Hydrophilic Interaction Chromatography Methods for Prednisolone Acetate Determination in Their Pure and Tablet, Syrup Dosage Forms, *Plant Arch.*, 2020, **20**, 2807–2812.

67 O. G. Bhusnure, S. Gholve, B. Manoj, V. Todkar and P. S. Giram, Analytical Method Development and Validation of Prednisolone Sodium Phosphate by QBD Approach, *IOSR J. Pharm. Biol. Sci.*, 2015, **10**, 64–75.

68 M. Arabi, M. Ghaedi, A. Ostovan and S. Wang, Synthesis of Lab-in-a-Pipette-Tip Extraction Using Hydrophilic Nano-Sized Dummy Molecularly Imprinted Polymer for Purification and Analysis of Prednisolone, *J. Colloid Interface Sci.*, 2016, **480**, 232–239.